This is to certify that the
thesis entitled

A NUMERICAL STUDY OF IN-CYLINDER MIXTURE FORMATION
IN A LOW PRESSURE DIRECT INJECTION GASOLINE ENGINE

presented by

Yuxin Zhang

has been accepted towards fulfillment
of the requirements for the

Master degree in Mechanical Engineering

Harold J. Schock
Major Professor's Signature

7/1/07
Date

PLACE IN RETURN BOX to remove this checkout from your record.
TO AVOID FINES return on or before date due.
MAY BE RECALLED with earlier due date if requested.

DATE DUE	DATE DUE	DATE DUE

A NUMERICAL STUDY OF IN-CYLINDER MIXTURE FORMATION IN A LOW PRESSURE DIRECT INJECTION GASOLINE ENGINE

By

Yuxin Zhang

A THESIS

Submitted to
Michigan State University
in partial fulfillment of the requirements
for the degree of

MASTER OF SCIENCE

Department of Mechanical Engineering

2007

ABSTRACT

A NUMERICAL STUDY OF IN-CYLINDER MIXTURE FORMATION IN A LOW PRESSURE DIRECT INJECTION GASOLINE ENGINE

By

Yuxin Zhang

A KIVA-3V based numerical simulation has been performed to study the in-cylinder flow field and fuel mixture formation process in a 5.4L V8 3-valve low pressure direct injection gasoline engine. GRIDGEN, which is a commercial grid generator software program, was used to build a fine mesh for the single cylinder with over a half million computational cells configured in 50 blocks. To resolve the problems of fine moving mesh in KIVA-3V, a new rezoner methodology was implemented. Simulation results show that the effect of injector spray pattern, enabled by the use of multi-hole fuel injectors to achieve spray tailoring flexibility, is a key factor to improve the fuel charge homogeneity in the cylinder.

ACKNOWLEDGEMENTS

I would like to express my sincere appreciation to my advisor Dr. Harold Schock, his constructive guidance and suggestions. This research would not have been accomplished without his patience and diligent assistance throughout my master program.

I would also like to thank my thesis committee members, Dr. Jaberi, Dr. Brereton for their constructive opinion and comments.

My thanks are also extended to Dr. David Hung from Visteon cooperation, Dr.Yang from Michigan Tech University, Dr.Ramadan from Kettering University and Dr. Das from Delphi Company for their advices on GRIDGEN meshing.

Thanks for Andy Fedawa, Mayank from MSU-ARES for providing MTV data and the help on the tuning of input parameter

TABLE OF CONTENTS

LIST OF TABLES

LIST OF FIGURES

All the figures are printed in color

LIST OF APPENDICES

NOMENCLATURE

a	length (m)
b	width (m)
E	power (W)
h_{fg}	latent heat of vaporization (kJ/kg)
L	length (m)
M	mass (kg)
P	pressure (Pa)
MAP	Manifold Air Pressure
SOI	Start of injection
EOI	End of injection
ATDC	After top dead center
BTDC	Before top dead center
Itape	KIVA3V imput files
CAD	Crank angle degree

CHAPTER 1

INTRODUCTION

1.1 Background

Over the past 15 years, the development of gasoline direct injection (GDI) engine is receiving significant interest in the automotive industry. Compared with the currently practiced port fuel injection (PFI) engine, a GDI engine has the potential for significant improvements in fuel economy while maintaining higher power output This seemingly contradictory and difficult task can be achieved by the combination of two combustion modes. [1-3].

For high engine load conditions, injection during the intake stroke (early injection) requires a large spray angle and sufficient penetration for maximum air utilization. However, excessive penetration aided by intake air flow and low cylinder pressure can result in significant cylinder wall and/or piston wetting [4]. A well atomized spray is essential for homogeneous mixture formation prior to ignition.

For part load conditions, injection occurs during the compression stroke (late injection) to achieve adequate charge stratification for lean burn combustion, which is desired for its high thermal efficiency. During the compression stroke, the cylinder pressure and temperature increase with crank angle. The charge turbulence intensity increases substantially near TDC due to the collapse of the large scale flow structures resulted from the significantly reduced volume and complicated engine geometry inside the combustion chamber. This phenomenon tends to improve the fuel droplet evaporation and air-fuel mixing. However, the increased air drag causes rapid deceleration of fuel droplets and increases the probability of droplet coalescence and the formation of large droplets.

With these modes, GDI engines must achieve the following: idle and light-load combustion stability and hydrocarbon control; best fuel economy in the light to medium load and speed ranges typical of normal driving cycles; best full load torque curve. Precise control of both airflow and fuel delivery is crucial to GDI engines' success. [1-3]

The performance of a direct injection gasoline engine (GDI) is highly dependent on the quality of the air-fuel mixture preparation. This is of particular importance when operating at a stratified charge condition, where the ideal mixture distribution would be a stoichiometric region around the spark plug, surrounded by air. To achieve this ideal situation over a wide range of speeds and loads is extremely difficult, requiring an understanding of the fuel spray, the in-cylinder air motion and their interactions. Experiments need to be conducted to evaluate the performance and the robustness of the turbulence models.

1.2 Thesis Objective

The efforts to solve for the technical difficulties in GDI engine have been practiced both experimentally and numerically. Modern techniques such as Computational Fluid Dynamics (CFD) will tremendously enhance the investigation process. Numerous programs and software have been devised and applied for pre- and post processing purposes. With the present and ever-increasing computing power, the use of CFD can efficiently study the complex flow fields of the engines, and will be an essential technique to engine research and development.

The main task of this project is to provide a numerical simulation of the intake flow field and the mixture preparation process in a 5.4L V8 3-valve low pressure direct injection gasoline engine. It also aims to compare the numerical result to the flow field measurements from Molecular Tagging Velocimetry and high speed visualization at the Automotive Research Experimental Station at Michigan State University [5].

1.3 Thesis outline

The numerical simulation consists of 2 major parts, including the engine in-cylinder model development and engine cycle flow field analysis with fuel injection. This part is excerpt from the part of the project proposal by Dr.David Hung in Visteon.

Part 1: Engine In-cylinder Model Development

A single cylinder model of the engine has been developed to include the parts of the intake and exhaust ports with valves, and combustion chamber, containing approximately 560,000 cells (at bottom dead center). The following data are provided with from CAD data or from experimental results:

- CAD data and dimensions for the bore, stroke, connecting rod length, piston pin offset, part of intake ports, part of exhaust ports, valves, cylinder head, piston shape, and spark plug location.

- Engine operating conditions such as engine RPM, and Intake and exhaust valve lift profiles and timings, and ignition timing. (Mathematical formulations of the intake & exhaust valve movements and piston movement).

- Modeling of the Charge Motion Control valve (only installed on one of the two intake ports)

- Inlet air condition (temperature and pressure) at the entry to the intake port.
- Wall temperature data for the intake port, exhaust port, cylinder head, liner, valves, and piston surfaces.

- Detailed information on the spray characteristics were provided by Visteon, including, droplet size, spray penetration, velocity, temperature, spray angle, spray offset angle, response time of the injector driver etc. Additional thoughts should be made when modeling the multi-hole fuel injector sprays.

Part 2: Engine Cycle Flow Field Analysis with Fuel Injection

After the geometry engine model is achieved, a fully three-dimensional unsteady flow simulation of the design should be performed for the engine cycle, starting from the intake stroke and running through the end of the compression stroke. Instantaneous flow field in the cylinder should be obtained and experimental flow field data using MTV can be used to correlate with the numerical results. Also, fuel injection should be included in the modeling effort. Modeling of the fuel injection event should begin at the instant when the fuel is injected in the cylinder.

The following specific information should be included:

- Fuel type should be specified, which includes either n-heptane, iso-octane or other generic gasoline fuel. Temperature dependent material properties will be used.
- Spray breakup and evaporation should be modeled using conventional Lagrangian tracking model.
- Conventional two-way coupling should be employed when modeling the fuel spray in a gaseous flow. The liquid and gas phases are fully coupled for mass, momentum, and temperature. Alternatively, a simpler one-way coupling from the droplets on the gas flow should be employed if possible. Droplet break-up and drop to drop collisions should be modeled.
- Droplets impacting a wall should also be modeled as spray impingement on the wall or piston top can form a liquid film on the liner surface.
- Wall heat transfer will be calculated which takes into account the compressibility of the gas.

The following outputs from analysis should be obtained:

- Three-dimensional flow field in the tumble plane (vertical) and swirl plane (horizontal), and with and without fuel spray, in the cylinder during the cycle including instantaneous development
- Charge air motion through the intake and exhaust valves during valve overlap.
- Details of the mixture formation, with the fuel spray evaporation taken into account. The air fuel mixture can be represented by using the distribution of Air-Fuel ratio. Also of interest is the fuel vapor distribution in the cylinder.
- Variation of in-cylinder fuel charge distribution and homogeneity by tailoring different spray characteristics should be documented in a quantitatively manner.

CHAPTER 2

LITERATURE REVEIW

Before the 1970's, engine researchers have primarily relied on experience, test results, and crude analyses based on empirical formulations to make final designs, which made the design processes were expensive and inefficient. Usually, empirical formulations could only provide zero dimensional or One-dimensional understanding of the flow conditions. The design based on empirical formulations could not meet the requirement of fuel economy and emission standards, which requires a more effective control of the combustion process.

Internal combustion engines are generally featured by unfavorable working conditions like reciprocating pistons and valves, high speed operations and high temperature of the working fluids, all of which greatly increased the difficulty of the transient and accurate flow measuring inside the cylinder. In the past two decades, high speed visualization and laser aided in-cylinder measuring [6] have gained great advancements, but there is still a long way to have accurate measurements of some local flow conditions and parameters. Also, the testing, though more accurate and reliable, is still a complicated process with a long developing period.

Over the past decades, with the development of mathematical models and computer resources[7,8] Engine simulation, featured by the combination of Computational Fluid Dynamics (CFD) and chemical kinetics has become an attractive and useful technique in most combustion industries because it has the potential to describe the flow physics inside a combustor.

In addition, numerical simulation can also reduce the number of design iterations by providing insight changes of design parameters or geometrical features, which have the characteristics of the flow in the combustor. Over the past decade, some successful simulations of turbulent fluid flow using CFD technique could provide an essential framework for combustor designs. [9,10]

Turbulent engine flows are highly anisotropic due to the complex geometry, wall effects, flow rotation (swirl), internal separation, etc. Therefore, to properly simulate the flow field inside various types of engines, a higher-order turbulence model should be used. The most widely used turbulence model in advanced CFD codes is the $\kappa - \varepsilon$ model.

This is because this model is very easy to implement. It requires relatively less CPU and memory resources compared with Reynolds stress formulations and direct numerical simulations (DNS). It does, however, have considerable drawbacks for use in resolving flow with high gradients of velocity and swirl. [11]

Despite of the advantages of the $\kappa - \varepsilon$ model, it has a tendency to yield inconsistent and diffusive results for complex flows because of its isotropic nature in modeling eddy viscosity.

The thesis focuses more on the building of computational mesh, the original $\kappa - \varepsilon$ model is still used as the model for simulation.

CHAPTER 3

PROBLEM SPECIFICATION

3.1 Engine Configuration

As shown in the Figure 3.1, the engine configuration includes a pent-roof combustion chamber, 2 intake valves with tilting angles of 5.1 degrees, an exhaust valve with a tilting angle of 5.8 degrees, and an optional charge motion control valve (CMCV) installed inside of one of the intake valve. Further engine specifications are listed in table 3.1 and table 3.2.

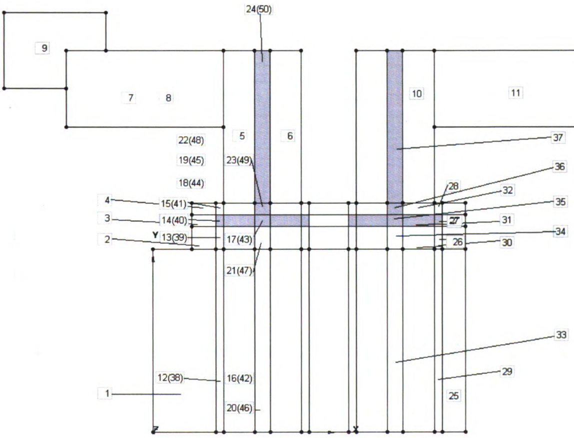

Figure 3.1 Engine block template, the bracketed blocks are created by copy subroutine in K3prep

Like most direct injection spark ignition engines, this 3-valve pent-roof engine has a complicated geometry which greatly increases the difficulty of meshing building.

Table 3. 1 Modeling Parameters and Conditions for Ford 5.4L 3 Valve Single Cylinder Engine

Component	Descrpition
Intake Fixed Ambient	T = 298
	P = 1
	D = 6
Exhaust Fixed Ambient	T = 650
	P = 0.67
	D = 5.7
Intake Runner	LD = RD = 4.8
	LN = 38.1
Intake Port	LD = 3.7
	RD = 3.185
	LN = 7
	CT = 2
Cylinder	Bore = 90.2 mm
	Stroke = 105.8 mm
	Con Rod = 198 mm
	Comp Ratio = 11
Note	
D	Diameter [D]
LD	Left Diameter [cm]
RD	Right Diameter [cm]
LN	Length [cm]
CT	Count
T	Initial Temperature [K]
P	Initial Pressure [bar]

Even for the initial mesh building process, it still requires a lot of insight into both the KIVA3V preprocessing and the mesh generator GRIDGEN. The major difficulties include:

- The narrow clearance between the valves and the cylinder wall resulting in great differences in sizes between the neighboring grids, which are undesired for CFD simulation (Figure 3.2)

Table 3.2 Valve lift profiles of the 3 valve engine

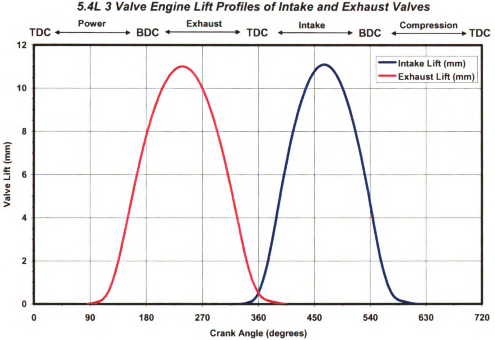

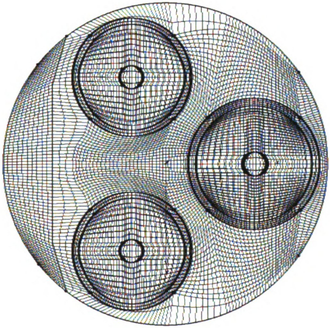

Figure 3.2. Actural mesh for the block1 in z direction

- Complicated side geometry of the pent roof, which consists of 200 facets and increases the difficulty of meshing greatly, especially for the hexahedral logical mesh adapted by KIVA3V.

- Complicated top geometry of the combustion chamber, which makes the building of the 1-layer top block (block 4)very difficult

- Complexity of valve profiles, the deep scallop in the exhaust valve, which has been a great challenge for mesh building and rezoning

Also, the thickness of the valves (about 2.5 mms) has made the one-layer block 3 considerably thick comparable with the neighboring layers in block4 and block2. Due to the inherent limitation of KIVA3V code, the block 3 consists only one layer. For a meshing of half a million of cells, the cells in this layer have been considerably huge and may greatly increase the time and difficulty for the code to arrive converging.

Charge motion control valve (CMCV), is a flow control device installed at the intake ports to increase the swirl motions inside the combustion chamber.

CMCV is usually activated at part load to improve the quality of the fuel-air mixture preparation. Thus it can increase the stability of idling for a direct injection engine.

However, CMCV is usually deactivated at full load or high rpm conditions. The increased piston speed has contributed greatly to the generation of turbulences. Also the early injection has also increased the homogeneity of the mixture. The mixture preparation quality has been satisfied and no further swirl motion is needed. The possible choking effects generated from the activation of CMCV could limit the flow rate. CMCV is deactivated at high rpm conditions.

KIVA3V has an option to exert an initial swirl motion inside the cylinder by adjusting the parameter "swirl", an option included since KIVA-2 was developed. Ford Company has provided a measurement of the swirl ratio generated from the activation of CMCV [21]. In this project, extra simulations at part load are performed to study the effects of CMCV. The comparison was performed between the 2 simulations: simulation based on the geometry with CMCV deactivated and an initial swirl ratio of 2.1 and simulation based on the geometry with CMCV and an initial swirl ratio of 0. The geometry of the CMCV and parameters are in Figure 3.3 and Table 3.3

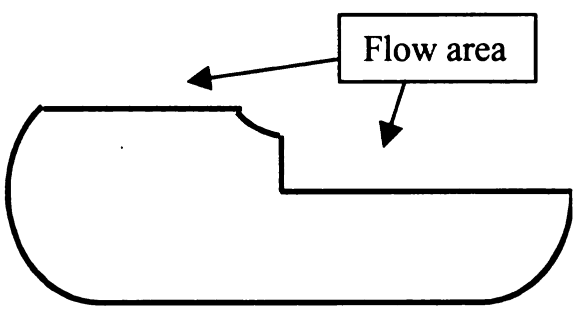

Figure 3.3. Geometry of charge motion control valve (CMCV)

Table 3.3 CMCV specifications

	CMCV Open		CMCV Closed	
	Standard Cam Timing	50° Cam Retard	Standard Cam Timing	50° Cam Retard
Tumble Ratio	0.3	0.9	1.2	1.2
Swirl Ratio	0	0	2.1	1.3

CHAPTER 4

CODE SETUPS AND COMPUTATIONAL MESHES

4.1 KIVA-3V $\kappa - \varepsilon$ Model Computations

The KIVA-3V [Amsden, 1997] computer code is the latest version of the KIVA family of CFD codes developed by Los Alamos National Laboratory (LANL), and is used worldwide among the engine research and development communities. It solves transient, two- and three-dimensional, chemical-reactive fluid flows with liquid-fuel spray. The turbulence models in the code include both the standard and RNG-variant $\kappa - \varepsilon$ models. [12-14]

The original Kiva3v obtained from Kettering University was a Linux system based code. Due to the limitation of Linux system in access, editing, simulation visualization and data transmission, the code was modified to be compatible with a Windows operation system.

The original version of KIVA-3V has been decomposed into 114 subroutines. Subroutine SETUP was modified to read the grid geometric information. Subroutine NEWLOCXYZ was added to replace original node information in KIVA Indexing. The flow diagram for the KIVA3-V program is listed in [12]

4.2 KIVA indexing and Plot3D indexing

The cooperation of Commercial grid generator GRIDGEN® and KIVA code inevitably involves the transform of mesh storage structure between the unique KIVA indexing notation system and the popular Plot3d indexing system.[15-18]

After building the mesh in GRIDGEN® exporting them in .grd files in Plot3D format, the grid information should be imported to KIVA3V code. The general idea is to replace the coordinates of the grid points assigned by K3prep mesh with the GRIDGEN® mesh. This process happens after the original single blocks are built and reshaped p while before the patching subroutines are called. Reshaping information are still provided in the iprep files, while the reshaping process in K3prep is virtually void since all the geometric information has been overlaid by the GRIDGEN® mesh.

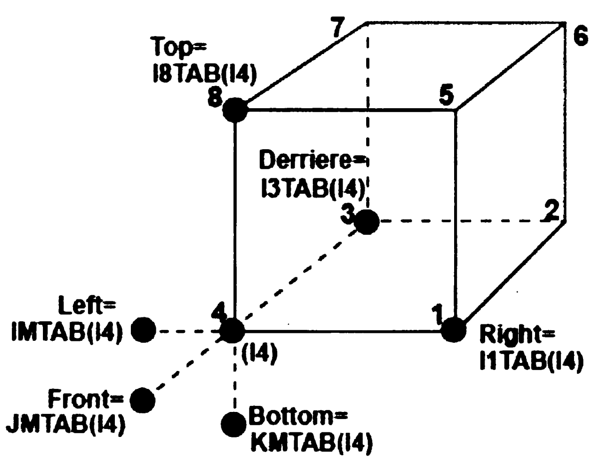

I1 = I1TAB(I4)
I2 = I3TAB(I1)
I3 = I3TAB(I4)
I5 = I8TAB(I1)
I6 = I8TAB(I2)
I7 = I8TAB(I3)
I8 = I8TAB(I4)

Figure 4.1(a) Kiva indexing notation system

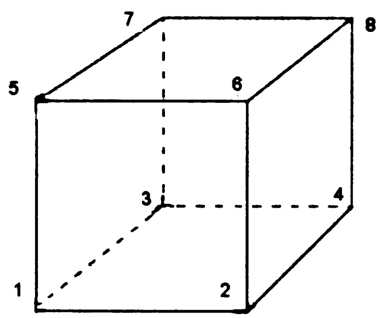

Figure 4.1(b) Plot3D indexing notation system

The graphic illustration of KIVA indexing notation and Plot 3D notation could be found in Figure 4.1.

4.3 Methodology of Structured Mesh Generation

Mesh preparation has been a bottleneck for CFD simulations of in-cylinder phenomena of internal combustion engines. The challenge mainly comes from two aspects: geometry complexity and moving mesh. Complex geometry makes the initial mesh generation difficult, while the moving piston and valves promote the need to re-mesh the computational domain for different piston and valve positions. In this work, a methodology has been developed for rapid mesh generation and dynamic mesh management with moving valves for internal combustion engines. A novel rezoner has been implemented to solve the moving mesh problems for this specific pentroof engine.

With the advancement of computer technologies and understanding of basic physical phenomena, 3-D simulation has played more and more important roles in the internal combustion (IC) engine development. Two of the important aspects of a 3-D simulation are the accuracy and user interaction time. The accuracy is mainly determined by the sub-models and numerical algorithm. Mesh generation is the major part of the user interaction, which could take up to 80% of the total work time. For 3-D simulation of IC engines, the challenge for mesh generation is its geometry complexity and moving piston and valves. The geometry complexity makes it difficult to generate the initial mesh for an engine design from a CAD file.

The initial mesh is the mesh corresponding to a piston and valve position. For the KIVA simulation, the valves could be either at the maximum life or fully closed. In our case, both the valves are set as closed. For all the cases, the valves are set as closed when the lifts are less than 0.4 mm [Figure 4.2]. Once the initial mesh is built, the computation domain is changing as the piston and valve move. This promotes the need for a robust dynamic mesh management algorithm to ensure the mesh quality during the valve and piston moving process.

Among IC engines, direct injection stratified charge spark ignition engine has inherently been one of the most complicated cases for mesh generation with its complicate bowl-in-piston geometry and piston protrusion above the head face once piston is at Top Dead Center(TDC). This thesis will focus on the mesh generation for Direct Injection Spark Ignition (DISI) engines.

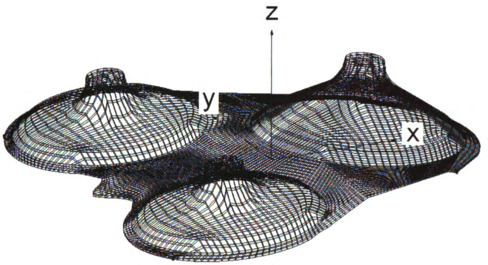

Figure 4.2(a) Single layered block4 with a thickness of 0.4mm

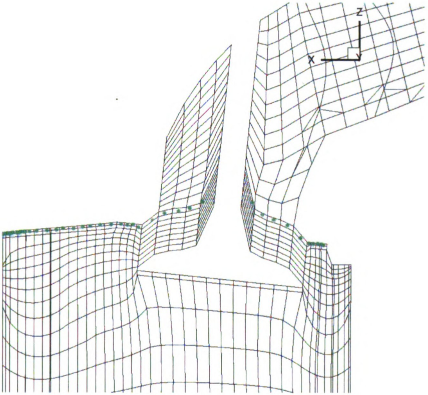

Figure 4.2(b) Deformation of block4 in the rezoning process

Initial mesh generation along with KIVA-3(V), there is a pre-processor called K3PRP. K3PRP has been applied for simple or simplified engine geometry. In K3PRP, the input of engine geometry is in text format either in a form of function or sets of discretized points of the surfaces or curves. Time consumption is another concern of K3PRP. In order for 3-D simulation to be an engineering tool, the mesh must have high geometry fidelity, and the mesh generation process needs to be very efficient.

The import of GRIDGEN® to KIVA3V requires a modification of K3prep. The general idea is to replace the coordinates of the grid points assigned by K3Prep mesh with the GRIDGEN® mesh. The details of the modification process would be stated in Appendix A.

4.4 Rezoning Process

In general, commercial software has high fidelity. The mesh could fit to the geometry very well. The interface includes the boundary condition, volume and surface flags setup. A case sensitive mesh topology has been developed for several typical engine geometry into several simple zones. In KIVA3V, they are defined as a block identity value named IDREG. The principle of decomposition is to divide the complicated combustion chamber into several different zones with either simpler geometry or less

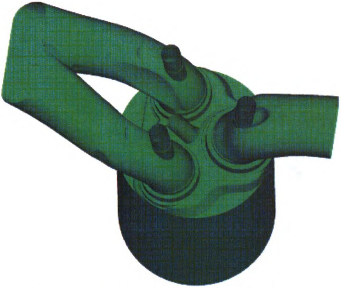

Figure 4.3 3-Valve Direct Injection Engine Geometry

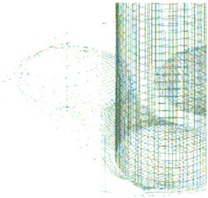

Figure 4.4 (a) Before local adjustment

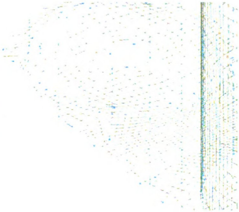

Figure 4.4 (b) After local adjustment

mesh movement. That is, in some zones, the geometry is complicated, but the mesh will not move much during the computation process. The mesh in those zones is much

easier to handle. Once the mesh is generated with fair quality (positive volume), the mesh will stay in such way though out the entire computational process. For zones with moving boundaries, the geometry is made to be simple such as between two parallel surfaces. The mesh in those zones is not only easy to generate but also the mesh is easy to manage during the piston and valve moving process. Such efforts make the re-meshing process much more robust, efficient, and reliable[19].

The computational mesh was created by using GRIDGEN® [2001] and a modified version of the KIVA pre-processor (K3PREP) [Amsden, 1997] program. A three-dimensional Cartesian multi-blocked mesh was constructed by using GRIDGEN®. The mesh was then exported into the K3PREP program where all blocks were appropriately patched. This procedure not only allows the construction of any complex geometry, but is also efficient in the use of time and resources.

Initial mesh is defined here as the mesh before the rezoning subroutines is called when the valves are moving. A fine initial mesh is a premise for the start of simulation. K3prep is modified to output mesh before simulation starts, which provides a convenient check of the initial mesh quality. While the inverted cells reported in K3prep are still not visually accessible. However, the new version of Tecplot includes a speedy Kiva3V data loader, without which the determination of inverted cells would cost a lot of time. The engine's 3-valve geometry itself provides a challenge for the building of mesh. Local mesh relaxation and intensification is widely used over the whole mesh building process.

Moving mesh has always been a challenging problem in mesh generation. Further optimization of the initial mesh is performed to balance the deformation resulted from the moving of valves. Again the cooperation of K3prep and Tecplot [20] plays an important role in the process. For a further check of the inverted cells in the moving mesh, a GRIDGEN® oriented exporter for the inverted cells was plugged in the SETUP subroutines in the KIVA3V main program. A total of 12 major modified versions were done in the process to eliminate inverted cells, decreasing the number of inverted cells from about 200 to 0.

Chapter 5

MESH GENERATION

This appendix shows the grid generation process of the 3-Valve pentroof engine using GRIDGEN®. The template of the block configuration of the combustor is shown in Figure 5.3, which consists of two tilted intake valves, a tilted exhaust valves, pentroof combustion chamber and the cylinder.

This appendix will provide a detailed procedure of creating a multi-blocked structured grid for the engine geometry.

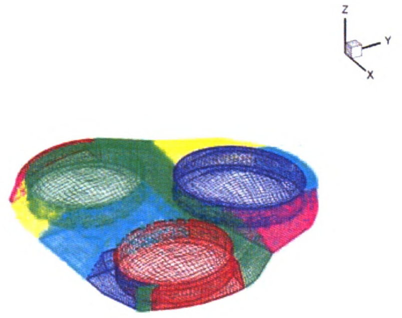

Figure 5.1(a) Block2 Divided

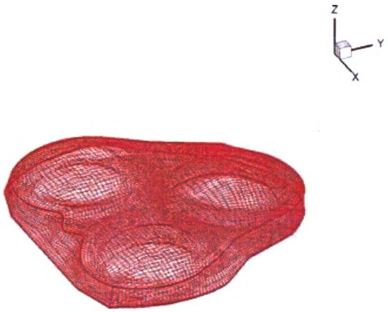

Figure 5.1 (b) Block2 joined

Transfinite interpolation (TFI) methods are usually used to create a surface mesh with inner constraint curves, for example, three inner circle in a square boundary as shown in Figure 5.1. However, GRIDGEN® divides the topology into 14 domains as labeled.

The basic geometry and parameters of engine are shown in Figure 5.2 and Table 5.1.

A plan view of the logical mesh, which is shown in Figure 5.3, helps creating the mesh, as well as indicating block numbers and vertex indices. In addition, it helps writing the block copying, reshaping, and patching commands in KIVA preprocessor (K3PREP).

Table 5. 1 Modeling Parameters and Conditions for Ford 5.4L 3 Valve Single Cylinder Engine

Component	Descrpition
Intake Fixed Ambient	T = 298
	P = 1
	D = 6
Exhaust Fixed Ambient	T = 650
	P = 0.67
	D = 5.7
Intake Runner	LD = RD = 4.8
	LN = 38.1
Intake Port	LD = 3.7
	RD = 3.185
	LN = 7
	CT = 2
Cylinder	Bore = 90.2 mm
	Stroke = 105.8 mm
	Con Rod = 198 mm
	Comp Ratio = 11
Note	
D	Diameter [D]
LD	Left Diameter [cm]
RD	Right Diameter [cm]
LN	Length [cm]
CT	Count
T	Initial Temperature [K]
P	Initial Pressure [bar]

5.1 Import IGES Database to GRIDGEN®

The solid model is first constructed by using the PRO/Engineer (Pro/E), which is then exported to an IGES format and eventually to the GRIDGEN® database. This section gives a brief introduction of importing the IGES database to GRIDGEN®.

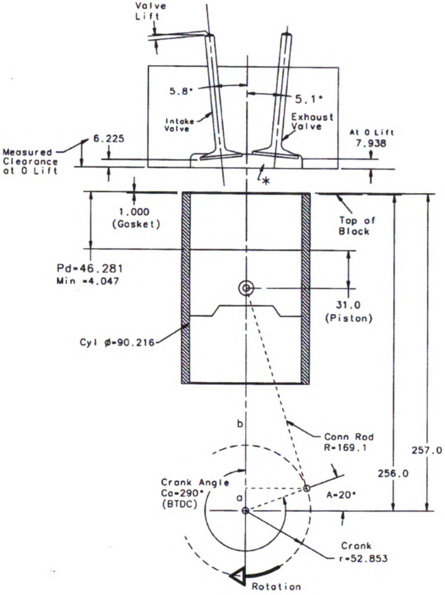

Figure 5.2 Engine basic configuration

Starting from the GRIDGEN® MAIN MENU:

1. Database

2. Import

3. Select 3Valve.igs from the Browser window

4. Open

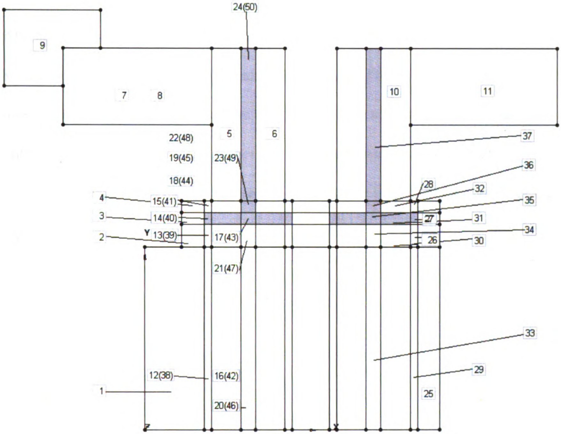

Figure 5.3 Engine block template, the bracketed blocks are created by copy subroutine in K3prep

5. Done

6. Select intake valve1.igs from the Browser window

7. Open

5. Done

6. Select intake valve2.igs from the Browser window

4. Open

5. Done

7. Select exhaust valve.igs from the Browser window

4. Open

5. Done

After importing the cylinder contour and the 3 valves, it is necessary to make sure that they are in proper position for KIVA3V calculation. The center of the bottom of the cylinder has to be at (0,0,0). The axis of the 3 valves have to be in the X-Z plane, with the intake valve titled by -5.8 degrees(counter clockwise) and the exhaust valves tilted by +5.1 degrees(clockwise). After the IGES database is adjusted, the Display window will look like Figure A.4

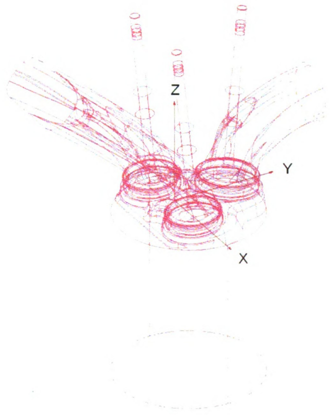

Figure 5.4 Engine geometry with valves installed

5.2 Logical Mesh

Figure 5.6 shows the logical mesh for the combustion chamber plane. Note that the bold grid lines indicate the block boundaries. For fine-grid density, there are total eight grid points along cylinder with a size of 73 grids in X-direction and 80 grids in and Y-direction, 54 grids in Z-direction. To redimension the connectors,

Starting from the CONNECTOR COMMANDS menu:

1. Redimensions
2. Select AB, CD
3. Enter 74
4. Select AC, BD
5. Enter 81
6. Done – Apply New Dims

The redimension processes of the connecters in other blocks have same procedures.

The finished topology and domain labels are shown in Figure 5.6.and Figure 5.7.

5.3 Creating Domains

Every domain is defined by four edges and the dimensions of each opposite edge should be exact. To create Domain 1,

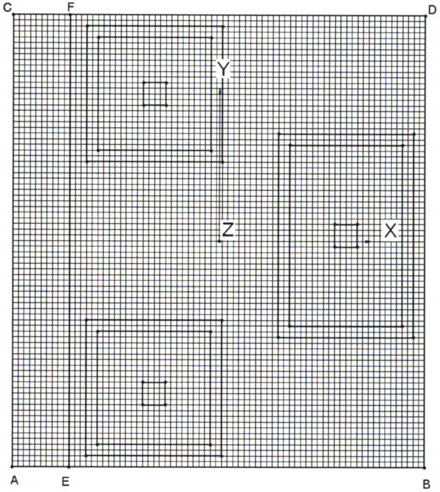

Figure 5.6. Logical mesh for the block1 in z direction

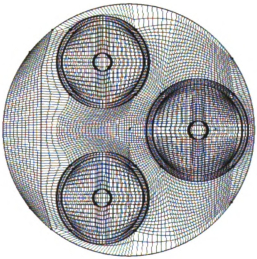

Figure 5.7. Actual mesh for the block1 in z direction

Starting from the MAIN MENU:

1. Domains

2. Create

3. Cell Type | ♦ Structured

4. Uncheck the Auto Next Edge and check the Auto Complete buttons

5. Assembly Edges

6. Select connector AB for the first edge of Domain 1

7. Next Edge

8. Select connectors AE and EB for the second edge

9. Next Edge

After defining second edges of the domain, GRIDGEN® will automatically complete the domain by selecting connector CF as the third edge because it has the same dimension to the first edge (i.e. connector AB); and selecting connector FA as the forth edge which has the same number of grid points to the second edge. Domain 1 has a dimension of 73×80 cells. Other domains are defined analogously. After all domains are created, the mesh will look like Figure 5.7

5.4 Creating Blocks

At least six faces are needed to construct a three-dimensional structured grid. Therefore, other five faces are created according to the coordinate system, i.e., left (ADHE), right (BCGF), front (ABFE), derriere (CDHG) and top (EFGH) faces as shown in Figure 5.8. The boundary topology needs to be created.

From the MAIN MENU:

1. Connectors

2. Create

3. 2 Points Connector

4. Place 3D cursor over point A

5. Add CG | by Picking on the IGES file

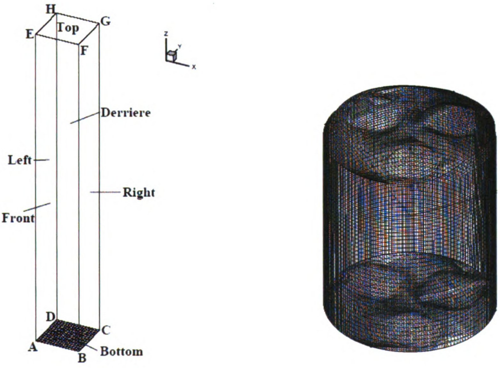

Figure 5.8 Domain boundary topology of a single block (Block 1)

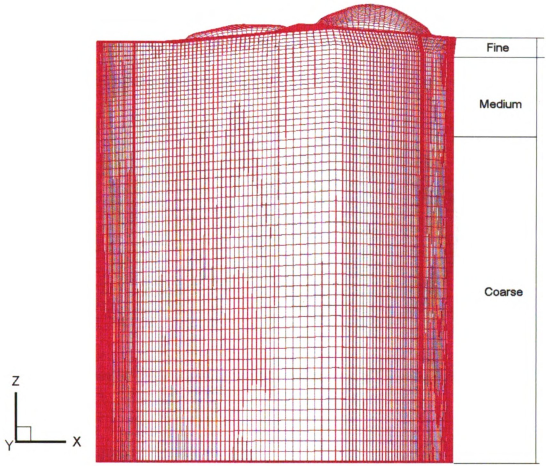

Figure 5.9 Mesh density variation on the Z-direction

8. Done

9. Done Creating Connectors

10. Redimensions

11. Select the connector AE

12. Enter 55

The block i, j, and k–direction grid lines are aligned into the positive x, y, and z–directions respectively by using Respecify ξ, η, ζ command. The burner block computational mesh is now done.

The intake block assembly has the similar configuration to the exhaust block assembly, and they can be done by using the procedure described above. Figure 5.10 shows the logical and computational meshes of the intake port.

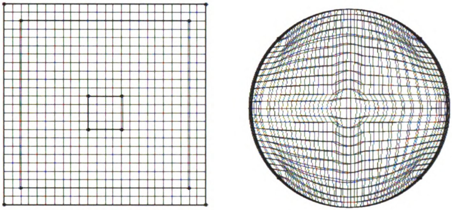

Figure 5.10 logical and computational meshes of the intake port

5.5 Block Reshaping

In our case, the meshing started from the valves to the larger blocks to be reshaped. Thus the blocks to be reshaped by K3prep have already contained the geometries of the shaping blocks inside.

As a result, the shaping process in K3prep has virtually already been done in the GRIDGEN meshing. The control of the reshaping process greatly reduced the chance of squishing some specific cells too much. The squishing of these cells may result in great difference in volume between the neighboring cells and involves possible problems for the spray modeling and internal energy equation's iteration.

In addition to the meshing for basic engine geometry, the engine meshing including the Charge Motion Control Valve (CMCV) is also built to study the CMCV's effect on charge motion. For CFD meshing, CMCV is a thin block vertical to the axis of intake runner. It blocks half of the flowing area in the intake runner. CMCV greatly increases the swirl ratio inside the cylinder.

Adaptive Meshing was also applied to the moving zone round the valves. In the regions swept by the valves as they move, the layers of grids have been shaped according the profiles of the valves. This effort greatly decreased the possibility of inverting cells in the snapping process.

Besides eliminating the ill-shaped cells with the aid of Jacobian Determinent Checker built in GRIDGEN at the building process of each block, a grid quality checker modified from relevant subroutines of the K3prep was also prepared. This grid checker checks the grid quality of each block in Plot3D format files according to KIVA's requirements. It also exports non-concaved cells in Plot3D format. The visualization of these cells in the early stage of meshing greatly reduced the work load. The necessary modification based on the visualization of the non-concaved cells in the building process increased the robustness of the meshing considerably. A total of 841600 cells in 50 blocks were generated, 552400 of which were retained after reshaping. As a result of the efforts above, only 103 non-concaved cells were reported by K3prep and no inverted cells were detected. Figure 5.11 shows the detected inverted cells of block4. They are visualized by GRIDGEN.

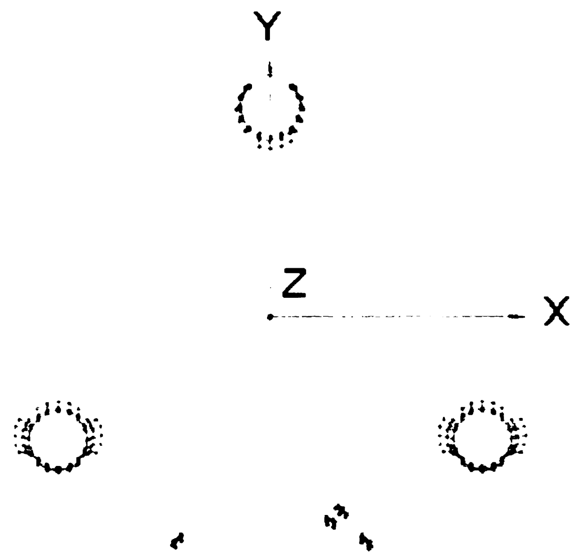

Figure 5. 11(a) Detected inverted cells

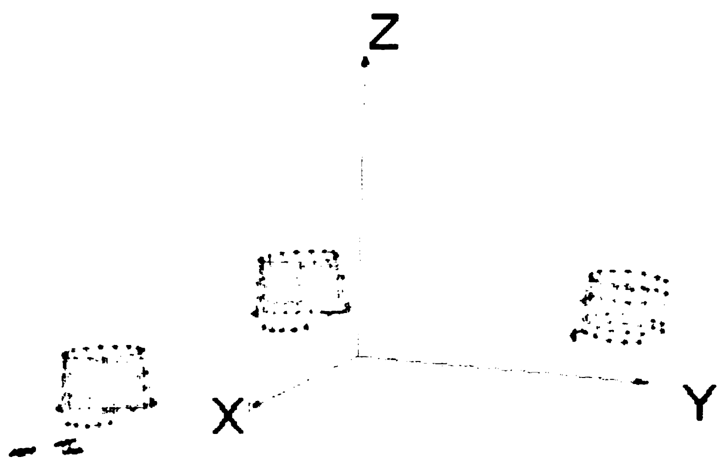

Figure 5. 11(b) Detected inverted cells

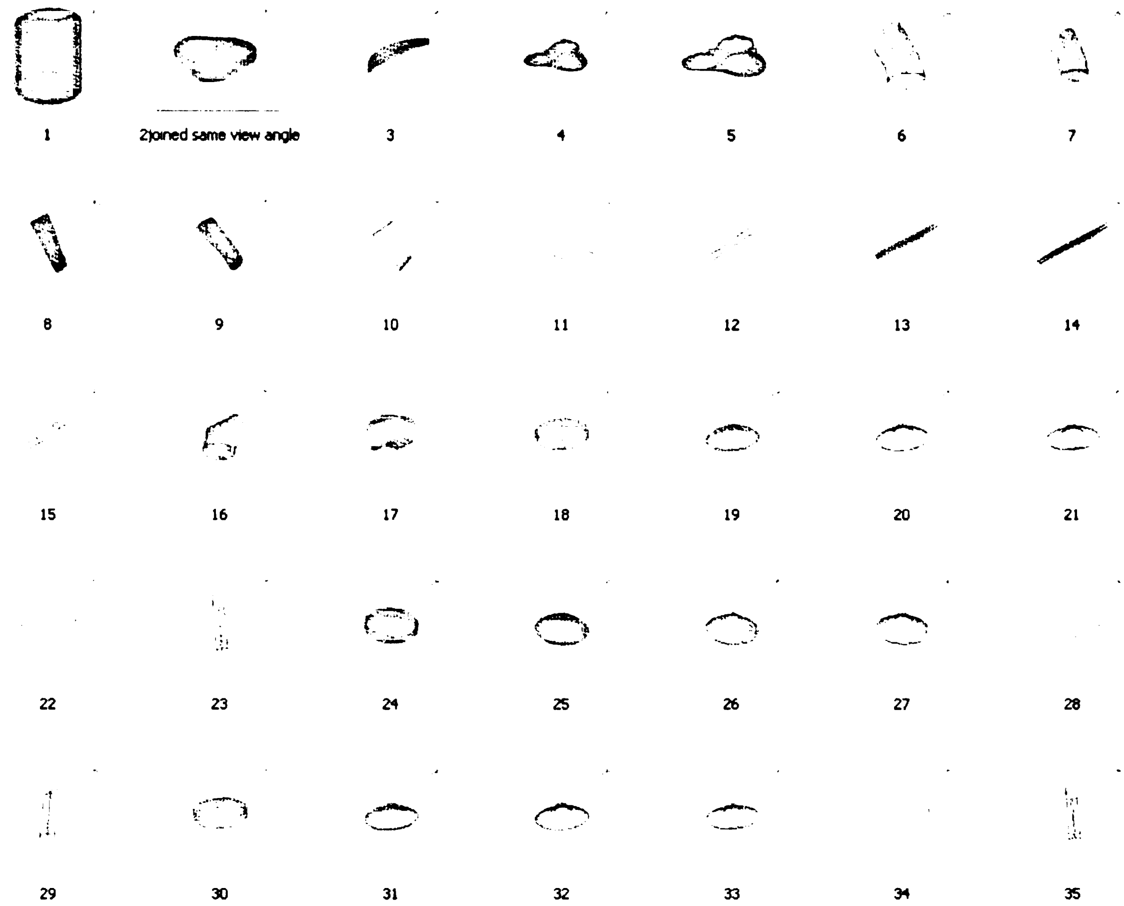

Figure 5.12 Computational meshes in blocks

5.6 Block Interconnection

The current version of GRIDGEN does not have a direct output format for the KIVA code. A modified K3PREP code sets up proper boundary conditions for moving valves and piston. The boundary conditions, reshaping and patching information are still provided in IPREP file.

The 50 blocks are saved separately in Plot.3D files. All of them are nominally saved as "block1", since they are output separately by GRIDGEN. Some manual changes on the blocks are necessary to number the blocks in right order. After the K3prep generating the blocks based on the information provided in IPREP, the blocks built by GRIDGEN are imported and rearranged in KIVA indexing notation.

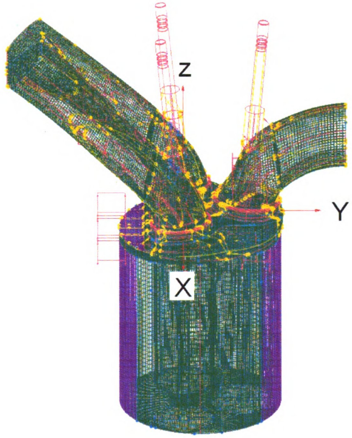

Figure 5.13 Overview of the Blocks after Patching and Reshaping

CHAPTER 6

RESULTS AND DISCUSSIONS

The primary goal of this study is to investigate the non-reacting flow fields inside the direction engine. The flow field and its impact on the preparation of mixture

6.1 Spray Parameters

Two sets of simulation are performed for part load at 1500RPM and full load at 2500RPM respectively, with 3 different core angles of spray, 3 different divergence angles, 3 different injection timings. Thus a total of 27 cases were simulated for each load mode. In each case, the mixture concentration, 3-D velocity field, temperature field, pressure field, oil film thickness are simulated and visualized. A total of 55,000 cells are built for the simulation with 50 blocks defined for the structured mesh.

The start of injection timing in Kiva3V is postponed by 13CAD (1.5ms) to accommodate the injection delay in the real operation conditions. Following values are used fuel injection parameters:

Total delay is 1 ms (injector pre charge) + 0.25 ms (Injector opening delay) = 1.25 ms.

For 1500RPM, the degree crank angle difference for 1.25 ms is about 11 degrees.

More detailed specifics of the engine configuration and the spray parameters could be found in Table 6.1 and Fig 6.1.

Table 6.1 Experimental and simulation parameters

	Parameters	
	Optical Engine	Kiva3V
Bore	90.216mm	90.216mm
Stroke	105.7mm	105.7mm
Injector Type	40/35/0(Spray angle/Axis angle/offset angle)	40/35/0(Spray angle/Axis angle/offset angle)
Injection Pressure	20Bar	20Bar
Injection Timing	330CAD BTDC (Intake Stroke)	319CAD BTDC (Intake Stroke)
Injection Duration	1.5ms/13CAD	1.5ms/13CAD
Engine Load	Part load:1500RPM/45.5KPa MAP;	Part load:1500RPM/45.5KPa MAP;
Initial Temperatures	345K(wall);345K(valve)	345K(wall);345K(valve)
SMR	15 microns	15 microns
Mass of Injection	15mg/cyc.	15mg/cyc.

A series of simulation results at the following operation conditions are listed in this paper based report. Other simulations results and some animation to feature the moving meshes and flow field visualization are included in the CD-ROM attached.

1500RPM (45 kar MAP): injection duration is 1.5 ms

Experiment: 330 deg SOI Before TDC / KIVA : 319 deg SOI Before TDC

Experiment: 300 deg SOI Before TDC / KIVA : 289 deg SOI Before TDC

Experiment: 270 deg SOI Before TDC / KIVA : 259 deg SOI Before TDC

Experiment: 1.5 ms for duration / KIVA : 13.2 deg for duration

Experiment: 1.5 ms for duration / KIVA : 13.2 deg for duration

Experiment: 1.5 ms for duration / KIVA : 13.2 deg for duration

6.2 Definitions

Some definitions are restated here as a recapitulation.

6.2.1 Velocity Magnitudes

The plotgmv files or otape12 files output by KIVA3V provide the velocity fields in x,y,z components. The velocity magnitude is defined as

Velocity Magnitude: $V_{total} = (U_2 + V_2 + W_2)^{1/2}$

Velocity in X-Y plane: $V_{uv} = (U_2 + V_2)^{1/2}$

Velocity in X-Z plane: $V_{uw} = (U_2 + W_2)^{1/2}$

The visualization of the velocity magnitude could be obtained by specify an corresponding expression of velocity magnitude for Tecplot.

6.2.2 Air-Fuel Mass Ratio

Since gasoline is a mixture with a variety of components, while the current version of KIVA3V doesn't support a multi-component fuel in its fuel library. Octane (C_8H_{18}) is used as the fuel for simulation. With a complete combustion of octane in the air, the oxidation equation is as follows:

$C_8H_{18} + 12.5O_2 + 47N_2 = 9CO_2 + 9H_2O + 47N_2$ (Equation 6.1)

With a molar mass of 114.228, the mass ratio of air to fuel is approximately 14.7.

6.2.3 Iso-surface of Ignitable Region

Iso-surface could be generally defined as a contour with a constant value of a scalar quantity. With the equivalence ratio of 1.0, the mass fraction of octane is calculated as 0.062 based on the oxidation equation. (Equation 6.1)

6. 3 Simulation Results and Discussions

Computations start from the 80° BTDC (-80 degree) and end at the compression TDC (360 degrees). The initial thermodynamic and turbulence parameters are specified to be uniform in the cylinder and in the intake port region separately. A pressure-boundary condition, based on the parameters of the Molecular Tagging Velocimetry(MTV) at the Engine Research Lab in Michigan State University, is imposed at the open end of the intake port runners. The modeled engine specifications at part load and spray parameters are listed in Table 6.1.

6.3.1 In-Cylinder Air Motion

The in-cylinder mean flow was analyzed first since the gas flow significantly impacts spray development and air-fuel mixing. In the following, details of in-cylinder air motion without fuel injection are described for an early injection mode. Figure 6.2-Figure 6.9 shows the velocity fields at three different crank angles during the intake and compression strokes.

The velocity vectors on the parallel plane to the piston surface indicates that the flow starts forming a swirl in the clockwise direction. As the piston moves down to BDC, a large scale swirling motion dominates the flow and the tumble motion has weakened. During the compression stroke, the dominant feature of the mean flow field continues to be the main swirl flow and the strength of the velocity vectors is nearly uniform. The tumble strength has not changed much from BDC.

6.3.2 Spray Pattern Effect on In-Cylinder Fuel Mixture Formation

Computations are performed to simulate the in-cylinder fuel/air mixing process of the engine under part load conditions In the part load operation mode at 1500 RPM, the start of the fuel injection (SOI) is 30° ATDC and the other engine operating conditions are kept the same values as other conditions. The injection duration is 13° CA (1.5ms). The mass for fuel per injection is 15 mg.

The injector specifications are listed on Table 1. The injector location, orientation, and multi-hole structure are illustrated in Fig. 11, in which the spray droplets are represented by the particles. Figure 6-1 shows the side-by-side comparison of the three injector sprays on fuel mixture distribution in thecombustion chamber at the engine part load condition of1500 RPM and a MAP pressure of 45.5 kPa absolute. At this part load condition, the fuel injection was set at a baseline level of 20 Bar. Initial speed of droplets was tuned as 50m/s.

The droplet distribution, mass fraction of fuel and the equivalence ratio across the chamber at various crank angles is shown in Fig 6.10-12 The equivalence ratio of 1.0 is represented as an iso-surface. When the fuel is injected at 41 CAD ATDC, the unity equivalence ratio (Massfrac $_{octane}$=0.062) near the spark plug indicates an ignitable value.

With a temperature of 350K on the cylinder wall and piston top, there is no ignitable region from the simulation. The phenomena could be explained as resulted from the low temperature of the cylinder wall and cylinder head, which greatly decelerated the process of evaporation and mixing.

With increase the temperature of 600K on piston top, 500K on the cylinder wall and 800K on the exhaust valve, the iso-surface of ignitable value at different crank angles is shown in Fig 6.12. It is noticed that the iso-surface breaks up into two pieces when approaching TDC.

6.3.3 Visualization of Simulation Results

Figure 6.1.1 High speed visualization of the In-cylinder droplets at 1500RPM/45.5kPa MAP/20 Bar Fuel Pressure/ SOI at 60 CA ATDC, by Courtesy of David Hung and Andy Fedewa

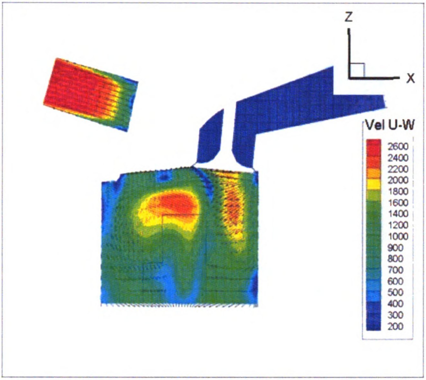

Figure6.1.2 Velocity field from simulation, with the MTV testing field circled; unit:cm/s

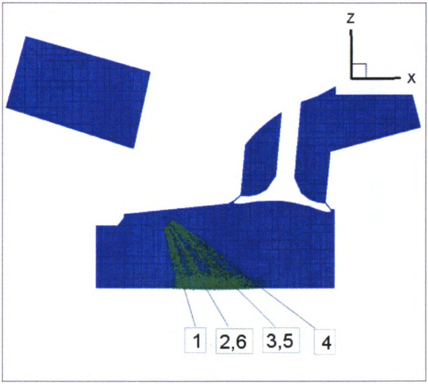

Figure6.1.3 Velocity field from simulation, with 6 nozzle spray numbered

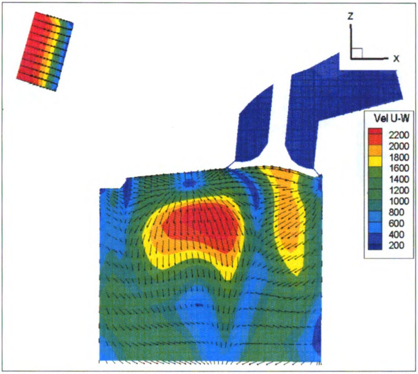

Figure 6.2.1 Velocity field from simulation (121CAD (ATDC)), tumble plane, CMCV deactivated, 1500rpm, unit:cm/s

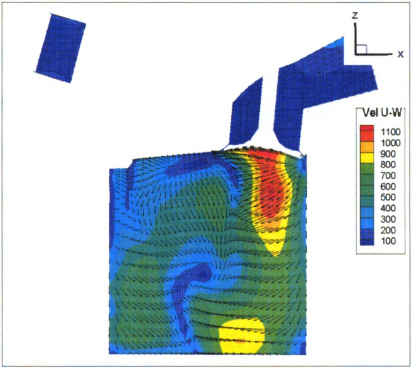

Figure 6.2.2 Velocity field from simulation (192CAD (ATDC)), tumble plane, CMCV deactivated, 1500rpm, unit:cm/s

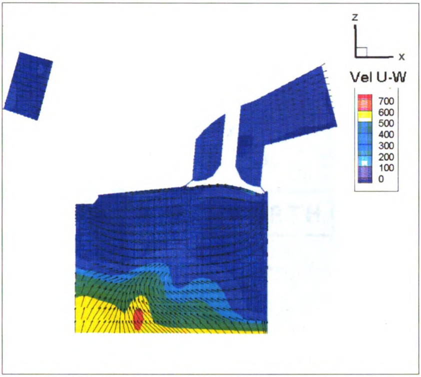

Figure 6.2.3 Velocity field from simulation (257CAD (ATDC)), tumble plane, CMCV deactivated, 1500rpm, unit:cm/s

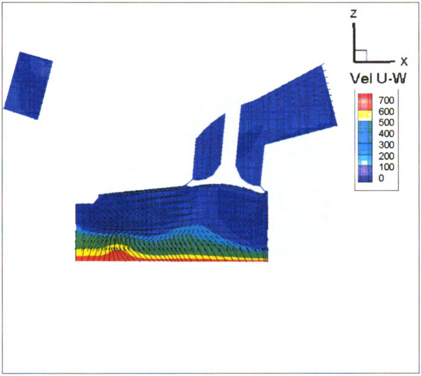

Figure 6.2.4 Velocity field from simulation (300CAD (ATDC)), tumble plane, CMCV deactivated, 1500rpm, unit:cm/s

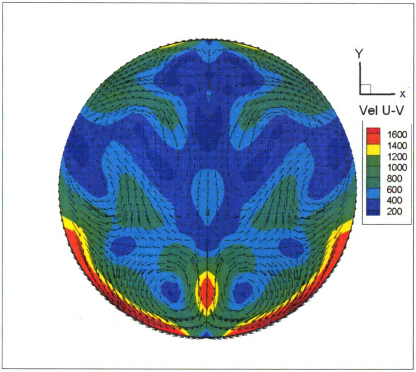

Figure 6.3.1 Velocity field from simulation (121CAD (ATDC)), swirl plane at 2.45cm from the head deck; CMCV deactivated, 1500rpm, unit:cm/s

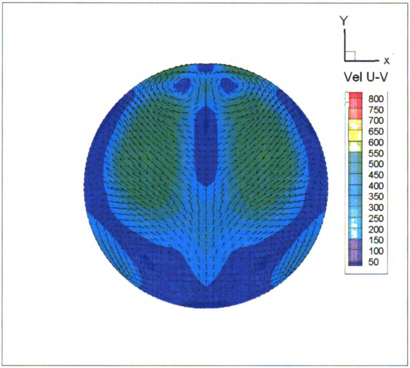

Figure 6.3.2 Velocity field from simulation (192CAD (ATDC)), swirl plane at 2.45cm from the head deck; CMCV deactivated, 1500rpm, unit:cm/s

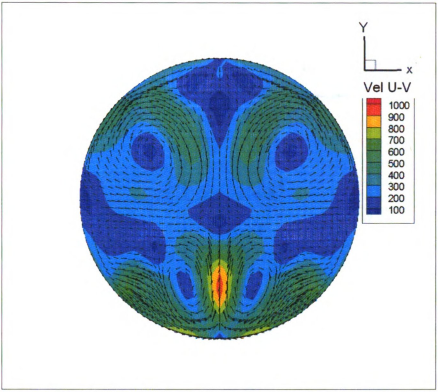

Figure 6.3.3 Velocity field from simulation (257CAD (ATDC)), swirl plane at 2.45cm from the head deck; CMCV deactivated, 1500rpm, unit:cm/s

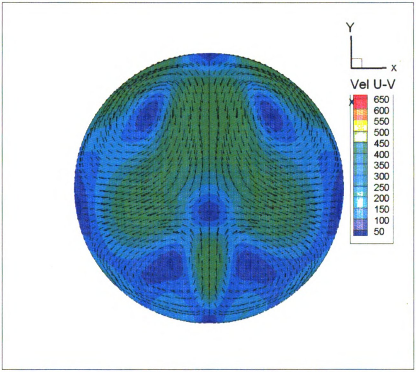

Figure 6.3.4 Velocity field from simulation (300CAD (ATDC)), swirl plane at 2.45cm from the head deck; CMCV deactivated, 1500rpm, unit:cm/s

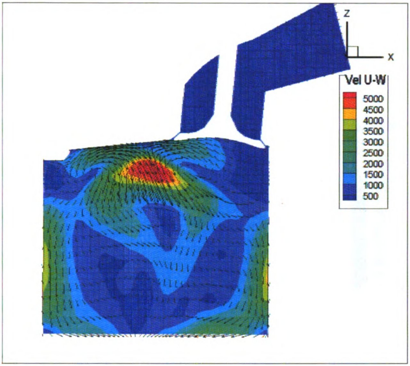

Figure 6.4.1 Velocity field from simulation (121CAD (ATDC)), tumble plane, CMCV activated, 1500rpm, unit:cm/s

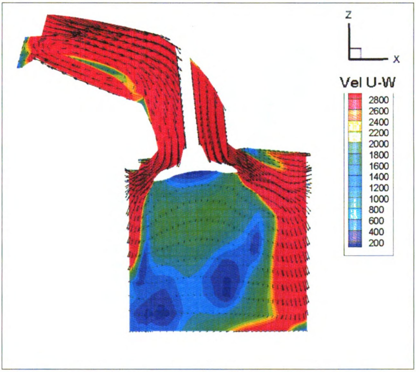

Figure 6.4.2 Velocity field from simulation (192CAD (ATDC)), tumble plane, CMCV activated, 1500rpm, unit:cm/s

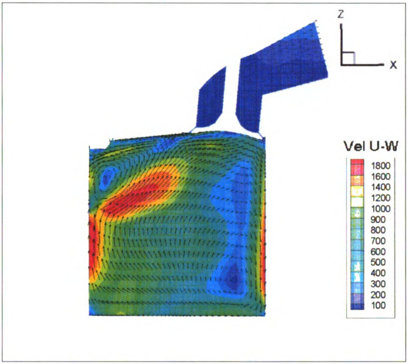

Figure 6.4.3 Velocity field from simulation (257CAD (ATDC)), tumble plane, CMCV activated, 1500rpm, unit:cm/s

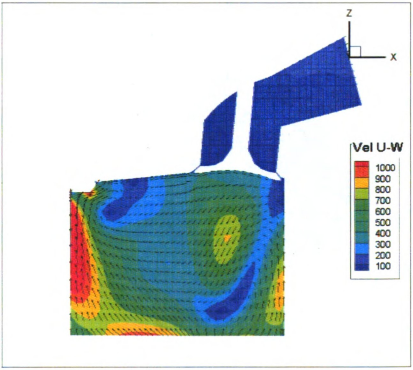

Figure 6.4.4 Velocity field from simulation (300CAD (ATDC)), tumble plane, CMCV activated, 1500rpm, unit:cm/s

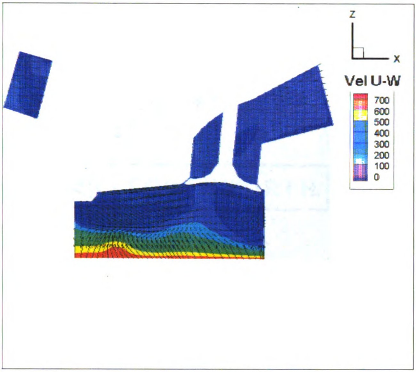

Figure 6.4.5 Velocity field from simulation (300CAD (ATDC)), tumble plane, CMCV activated, 1500rpm, unit:cm/s

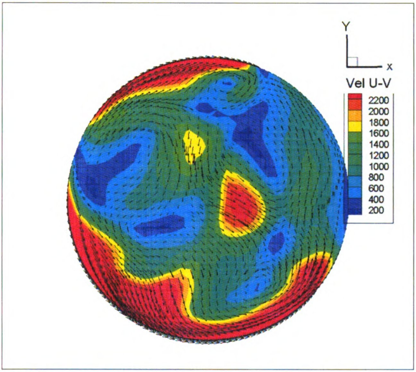

Figure6.5.1 Velocity field from simulation (121CAD (ATDC)), swirl plane at 245cm from the head deck; CMCV activated, unit:cm/s

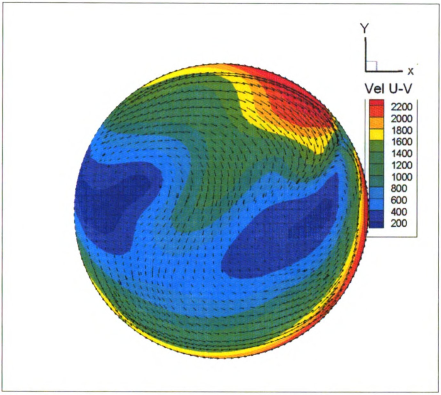

Figure 6.5.2 Velocity field from simulation (121CAD (ATDC)), swirl plane at 245cm from the head deck; CMCV activated, unit:cm/s

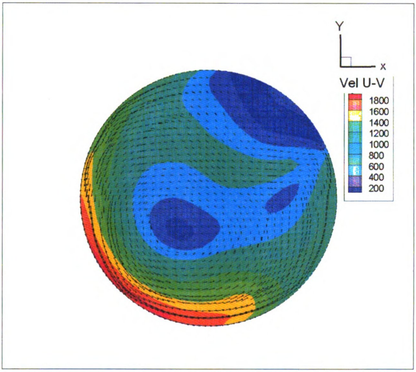

Figure 6.5.3 Velocity field from simulation (121CAD (ATDC)), swirl plane at 245cm from the head deck; CMCV activated, unit:cm/s

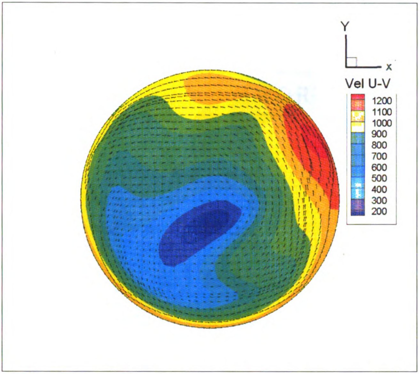

Figure 6.5.4 Velocity field from simulation (121CAD (ATDC)), swirl plane at 245cm from the head deck; CMCV activated, unit:cm/s

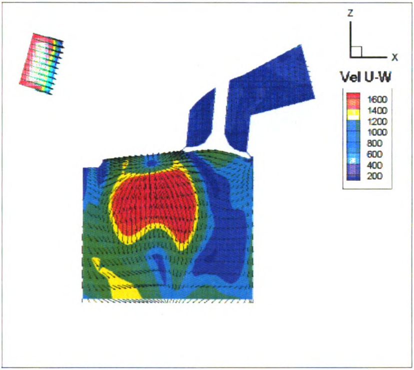

Figure 6.6.1 Velocity field from simulation (121 CAD (ATDC)), tumble plane, CMCV deactivated, 1500rpm, swirl=2.1,unit: cm/s

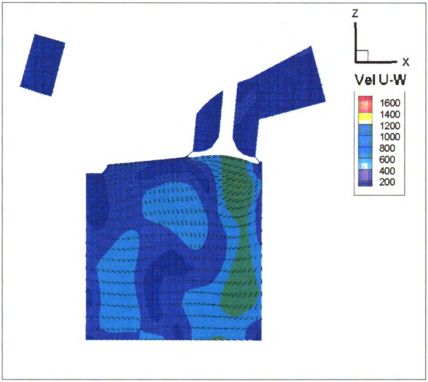

Figure 6.6.2 Velocity field from simulation (192 CAD (ATDC)), tumble plane, CMCV deactivated, 1500rpm, swirl=2.1,unit: cm/s

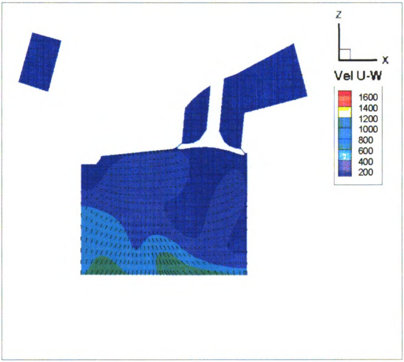

Figure 6.6.3 Velocity field from simulation (257 CAD (ATDC)), tumble plane, CMCV deactivated, 1500rpm, swirl=2.1,unit: cm/s

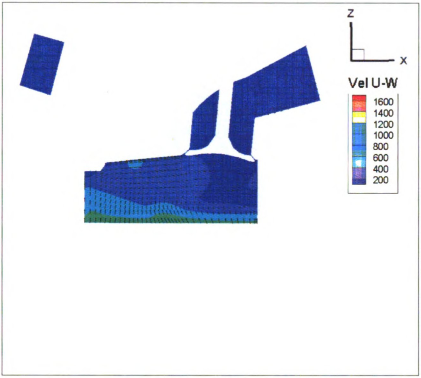

Figure 6.6.4 Velocity field from simulation (300 CAD (ATDC)), tumble plane, CMCV deactivated, 1500rpm, swirl=2.1,unit: cm/s

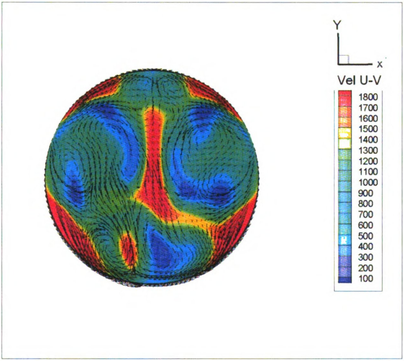

Figure 6.7.1Velocity field from simulation (121CAD (ATDC)), swirl plane at 2.45cm from the head deck; 1500rpm,swirl=2.1, unit:cm/s

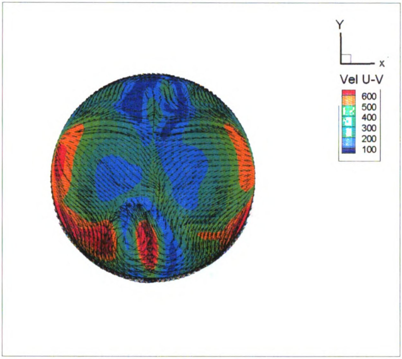

Figure 6.7.2 Velocity field from simulation (192CAD (ATDC)), swirl plane at 2.45cm from the head deck; 1500rpm,swirl=2.1, unit:cm/s

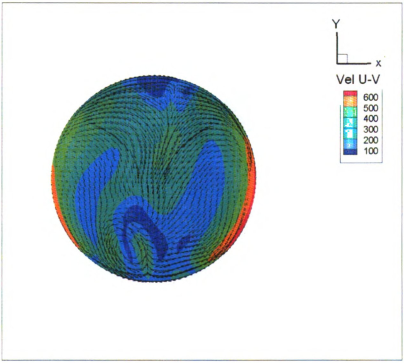

Figure 6.7.3 Velocity field from simulation (192CAD (ATDC)), swirl plane at 2.45cm from the head deck; 1500rpm,swirl=2.1, unit:cm/s

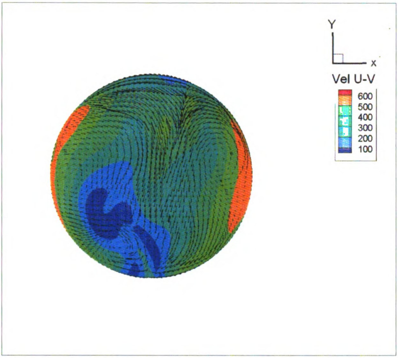

Figure 6.7.4 Velocity field from simulation (192CAD (ATDC)), swirl plane at 2.45cm from the head deck; 1500rpm,swirl=2.1, unit:cm/s

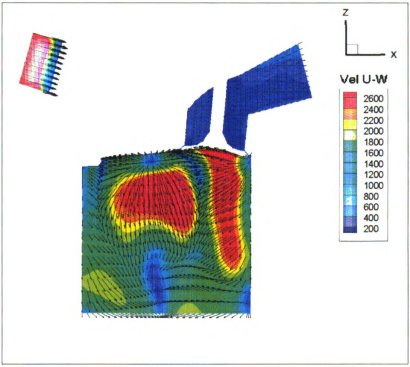

Figure 6.8.1 Velocity field from simulation (138 CAD (ATDC)), tumble plane, CMCV deactivated, 2500rpm, unit:cm/s

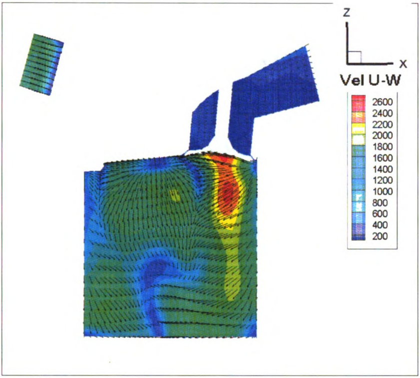

Figure 6.8.2 Velocity field from simulation (171CAD (ATDC)), tumble plane, CMCV deactivated, 2500rpm, unit:cm/s

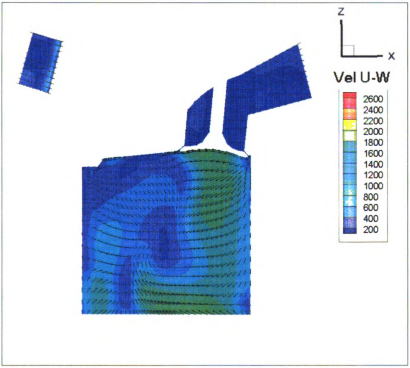

Figure 6.8.3 Velocity field from simulation (221 CAD (ATDC)), tumble plane, CMCV deactivated, 2500rpm, unit:cm/s

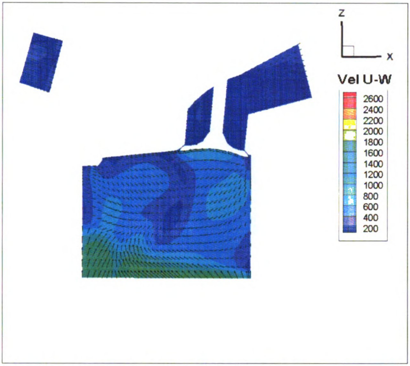

Figure 6.8.4 Velocity field from simulation (253 CAD (ATDC)), tumble plane, CMCV deactivated, 2500rpm, unit:cm/s

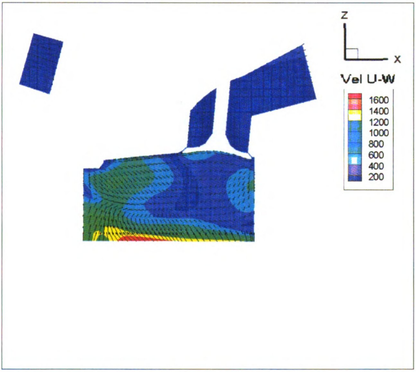

Figure 6.8.5 Velocity field from simulation (286 CAD (ATDC)), tumble plane, CMCV deactivated, 2500rpm, unit:cm/s

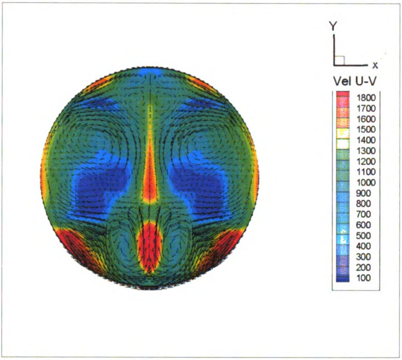

Figure 6.9.1 Velocity field from simulation (138CAD (ATDC)), swirl plane at 2.45cm from the head deck; 1500rpm,swirl=2.1, unit:cm/s

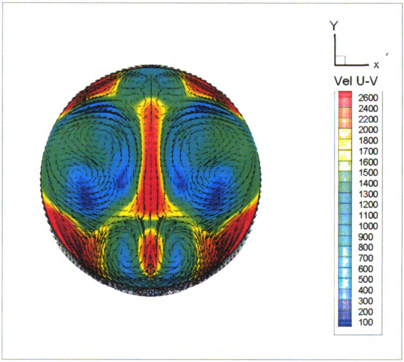

Figure 6.9.2 Velocity field from simulation (171CAD (ATDC)), swirl plane at 2.45cm from the head deck; CMCV activated, unit:cm/s

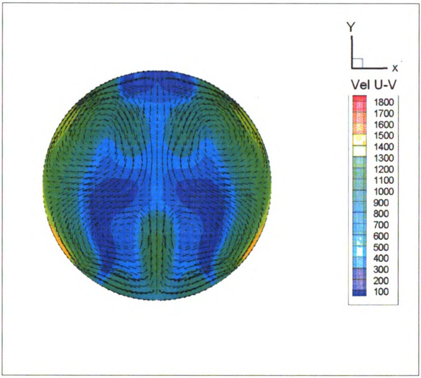

Figure 6.9.3 Velocity field from simulation (192CAD (ATDC)), swirl plane at 2.45cm from the head deck; 1500rpm,swirl=2.1, unit:cm/s

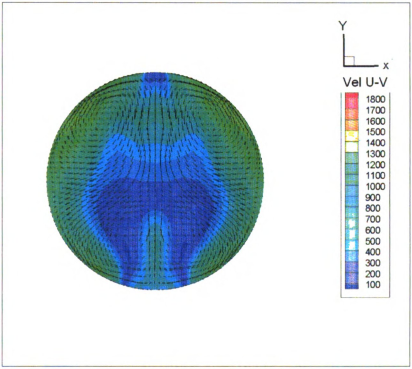

Figure 6.9.4 Velocity field from simulation (192CAD (ATDC)), swirl plane at 2.45cm from the head deck; 1500rpm,swirl=2.1, unit:cm/s

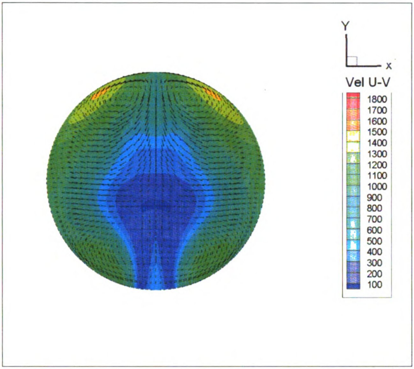

Figure 6.9.5 Velocity field from simulation (192CAD (ATDC)), swirl plane at 2.45cm from the head deck; 1500rpm,swirl=2.1, unit:cm/s

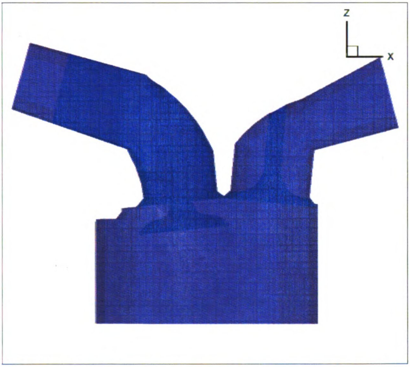

Figure 6.10.1 Gasoline droplets distribution 77 CAD (ATDC)

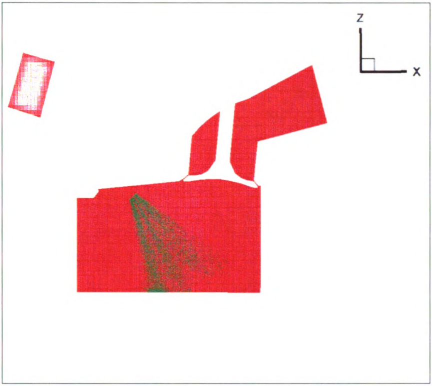

Figure 6.10.2 Gasoline droplets distribution 85 CAD(ATDC)

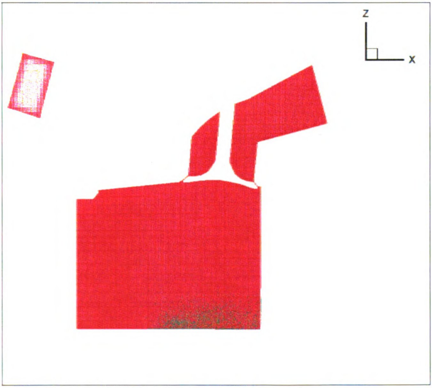

Figure 6.10.3 Gasoline droplets distribution 105 CAD(ATDC)

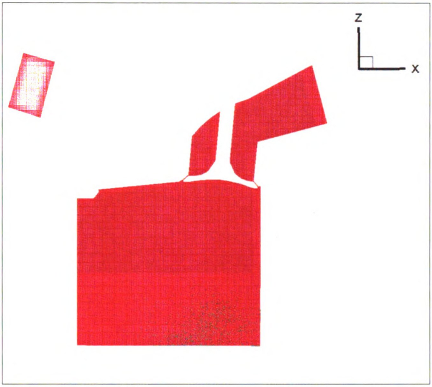

Figure 6.10.4 Gasoline droplets distribution 125 CAD(ATDC)

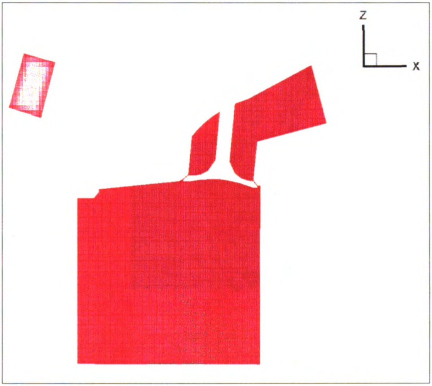

Figure 6.10.5 Gasoline droplets distribution 150 CAD(ATDC)

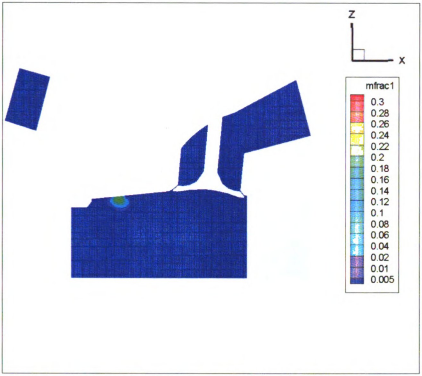

Figure 6.11.1 Octane molecular fraction (56CAD ADTC, 1CAD after EOI)

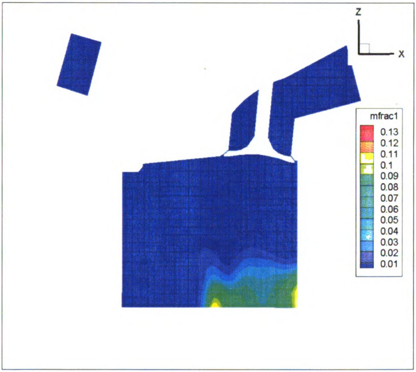

Figure 6.11.2 Octane molecular fraction (192 CAD ATDC)

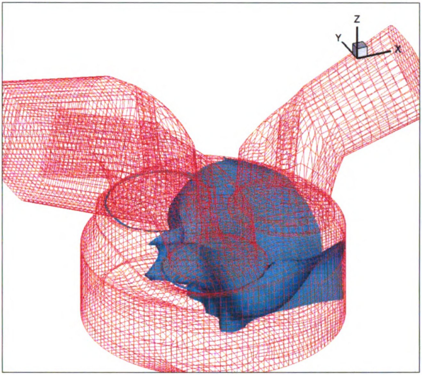

Figure 6.12.1 Computed equivalence ratio of 1.0 at 300 ATDC

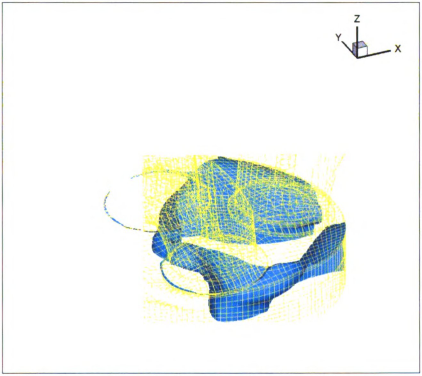

Figure 6.12.2 Computed equivalence ratio of 1.0 at 330 ATDC

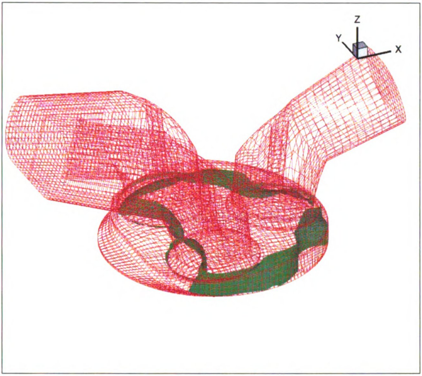

Figure 6.12.3 Computed equivalence ratio of 1.0 at 360 ATDC

Chapter 7

SUMMARY AND CONCLUSTIONS

7.1 Summary

A KIVA-3V based numerical simulation has been performed to study the in-cylinder flow field and fuel mixture formation process in a 5.4L V8 3-valve low pressure direct injection gasoline engine. GRIDGEN, which is a commercial grid generator software program, was used to build a fine mesh for the single cylinder with over a half million computational cells configured in 50 blocks. To resolve the problems of fine moving mesh in KIVA-3V, a new rezoner methodology was implemented. Simulation results show that the effect of injector spray pattern, enabled by the use of multi-hole fuel injectors to achieve spray tailoring flexibility, is a key factor to improve the fuel charge homogeneity in the cylinder.

The following is a list of what has been accomplished in this research:

- Decomposition and analysis of Kiva3v main code;
- Test run of the public simulations from Los Alamos;
- Simulation of the engine purely by K3prep+Kiva3V;
- Analysis and comparison of Kiva simulation results and MTV data;

- Studying the basis of Gridgen;
- Mesh generation using Gridgen;
- K3prep modification for reading Gridgen data and boundary condition set ups;
- Tuning of input parameters;
- Kiva Simulation of the engine on mesh generated from Gridgen;
- Analysis and comparison of Kiva simulation results and MTV data;

7.2 Conclusions and Recommendations for Future Work

The GRIDGEN-KIVA simulation of internal combustion engine has been a more complicated process than the commercial 3-Dimensionl CFD software such as Fluent or STAR-CD. With good meshing, the simulation has acceptable accuracy, while the original $\kappa-\varepsilon$ model included in KIVA3V could not provide simulation accuracy like the Large Eddy Simulation (LES). Recommendations on the future work has been listed as follows:

- Improved break-up and evaporation models could be implemented for the current mesh to improve the accuracy of the simulation of fuel-air mixing process.

- The program could be modified to be capable of parallel computing to have a full utilization of the advanced computation facilities like supercomputers

- The simultaneous measuring of the third velocity component should be measured in the experiment for more comprehensive result comparisons, such as magnitude of swirl velocity and turbulence kinetic energy.

- The high speed visualization in this thesis has been performed without combustion process. Thus the temperatures of the cylinder wall, cylinder head, valves and the top of piston have been much lower than the operating engine conditions. The slower evaporation of fuel results in extra impingement.

- KIVA uses a quasi-second order upwind (QSOU) and partial donor cell (PDC) schemes, which are monotone schemes and only first order accuracy, to calculate the convective transport equations. A higher order scheme, such as the Total Variation diminishing (TVD) scheme, should be incorporated into the code order to facilitate the construction of a more accurate computational model.

APPENDIX A

K3PREP MODIFICATION

K3PREP is a basic grid generator that is included in the KIVA package. It is capable to generate the simple geometries and to patch the blocks together in a straightforward manner. K3PREP read an input file named IPREP, which defined the shapes of the geometries and their boundary conditions. The size of the IPREP is depended on the complexity of the geometries. A more complicated mesh usually requires more blocks to be built.

GRIDGEN® is a grid generator software that has made extraordinary progress in the design process. It does not only reduce the enormous work for designing a complex geometry, but also produce a good quality mesh. GRIDGEN® exports the mesh to a volume grid file to produce ITAPE17 for the KIVA code. GRIDGEN® style volume grid file has a following format:

```
c.....number of grid points in block
    integer ni(nmax), nj(nmax), nk(nmax)
c.....define the size of the blocks
    real x(imax,jmax,kmax), y(imax,jmax,kmax), z(imax,jmax,kmax)
c.....block identification
    write(1) nblocks
    do mb = 1, nblocks
    write(1) ni(mb), nj(mb), nk(mb)
c.....output format
```

```
      write(1) (((x(i,j,k),i=1,ni(mb)),j=1,nj(mb)),k=1,nk(mb)),
      & (((y(i,j,k),i=1,ni(mb)),j=1,nj(mb)),k=1,nk(mb)),
      & (((z(i,j,k),I=1,ni(mb)),j=1,nj(mb)),k=1,nk(mb))
      end do
```

Additional subroutine named READGRID is added into K3PREP for reading the GRIDGEN® volume grid file and subroutine SETUP has been modified to tailor the specific needs.

```
c +++ yx-shalabh
c    do nn=1,19
c    write(65,*) nn, i4lfb(nn)
c    enddo
c    stop
c
      open(unit=3,file='verts')
      do 40 n=1,nlocxyz
c +++
c +++
      read (3,900) nblk1,indexi,indexj,indexk,xloc,yloc,zloc
c     indexi=indexi+1
c     indexj=indexj+1
c     indexk=indexk+1
      write(11,900) nblk1,indexi,indexj,indexk,xloc,yloc,zloc
c +++
      if(nblk1.eq.4.and.indexi.eq.7.and.indexj.eq.1.and.indexk.eq.2)
     * then
       write(*,*) "Exported"
      endif
c +++
```

```
      i4=i4lfb(nblk1)
      if(indexi.gt.1) then
       do 10 i=1,indexi-1
       i4=i1tab(i4)
 10   continue
      endif
      if(indexj.gt.1) then
       do 20 j=1,indexj-1
       i4=i3tab(i4)
 20   continue
      endif
      if(indexk.gt.1) then
       do 30 k=1,indexk-1
       i4=i8tab(i4)
 30   continue
      endif
      x(i4)=xloc
      y(i4)=yloc
      z(i4)=zloc
      ireshape(i4)=1
c yx-shalabh modified for creating  blocks
c     ireshape(i4)=0
c     write(66,901) nblk1,indexi,indexj,indexk,i4,x(i4),y(i4),z(i4)
c     stop
 40 continue
      return
c
 900 format(4i4,3f8.3)
 901 format(4(i4,2x),i8,3f8.3)
      end
```

APPENDIX B

KIVA Input Files

B.1 IPREP

```
 bore     9.0216
 stroke   9.0
 squish   1.58
 thsect 360.0
nblocks  37
 1 73 80 54  0  2  1  0
 4.5108 4.5108 -4.5108 -4.5108 4.5108 4.5108 -4.5108 -4.5108
-4.5108 4.5108 4.5108 -4.5108 -4.5108 4.5108 4.5108 -4.5108
 0.0    0.0    0.0    0.0    8.6150 8.6150 8.6150 8.6150
 2.0    2.0    2.0    2.0    1.0    2.0
-1.0   -1.0   -1.0   -1.0    0.0   -1.0
 2 73 80  7  0  2  1  0
 3.6000 3.6000 -3.6000 -3.6000 3.6000 3.6000 -3.6000 -3.6000
-3.6000 3.6000 3.6000 -3.6000 -3.6000 3.6000 3.6000 -3.6000
 8.6150 8.6150 8.6150 8.6150 8.6900 8.6900 8.6900 8.6900
 2.0    2.0    2.0    2.0    4.0    4.0
-1.0   -1.0   -1.0   -1.0   -1.0   -1.0
 3 73 80  1  0  4  1  0
 3.6000 3.6000 -3.6000 -3.6000 3.6000 3.6000 -3.6000 -3.6000
-3.6000 3.6000 3.6000 -3.6000 -3.6000 3.6000 3.6000 -3.6000
 8.6900 8.6900 8.6900 8.6900 8.7400 8.7400 8.7400 8.7400
 2.0    2.0    2.0    2.0    4.0    4.0
-1.0   -1.0   -1.0   -1.0   -1.0   -1.0
 4 73 80  1  0  4  1  0
 3.6000 3.6000 -3.6000 -3.6000 3.6000 3.6000 -3.6000 -3.6000
-3.6000 3.6000 3.6000 -3.6000 -3.6000 3.6000 3.6000 -3.6000
 8.6900 8.6900 8.6900 8.6900 8.7400 8.7400 8.7400 8.7400
 2.0    2.0    2.0    2.0    4.0    2.0
-1.0   -1.0   -1.0   -1.0   -1.0   -1.0
 5 20 20 26  0  5  2  0
 1.4925 1.4925 -1.4925 -1.4925 1.4925 1.4925 -1.4925 -1.4925
-1.4925 1.4925 1.4925 -1.4925 -1.4925 1.4925 1.4925 -1.4925
 8.7400 8.7400 8.7400 8.7400 14.0900 14.0900 14.0900 14.0900
 2.0    2.0    2.0    2.0    4.0    2.0
-1.0   -1.0   -1.0   -1.0   -1.0   -1.0
 6 20 20 26  0  5  2  0
 1.4925 1.4925 -1.4925 -1.4925 1.4925 1.4925 -1.4925 -1.4925
-1.4925 1.4925 1.4925 -1.4925 -1.4925 1.4925 1.4925 -1.4925
```

8.7400 8.7400 8.7400 8.7400 14.0900 14.0900 14.0900 14.0900
2.0 2.0 2.0 2.0 4.0 2.0
-1.0 -1.0 -1.0 -1.0 -1.0 -1.0
7 70 20 20 0 4 2 0
-4.0428 -4.0428 -7.4623 -7.4623 -2.1342 -2.1342 -6.45 -6.45
0.1000 2.7000 2.7000 0.1000 0.1000 2.7000 2.7000 0.1000
11.1969 11.1969 13.1794 13.1794 13.6397 13.6397 15.7900 15.7900
9.0 4.0 2.0 2.0 2.0 2.0
-1.0 -1.0 -1.0 -1.0 -1.0 -1.0
8 70 20 20 0 4 2 0
-4.0428 -4.0428 -7.4623 -7.4623 -2.1342 -2.1342 -6.45 -6.45
-2.7000 -0.1000 -0.1000 -2.7000 -2.7000 -0.1000 -0.1000 -2.7000
11.1969 11.1969 13.1794 13.1794 13.6397 13.6397 15.7900 15.7900
9.0 4.0 2.0 2.0 2.0 2.0
-1.0 -1.0 -1.0 -1.0 -1.0 -1.0
9 22 4 20 0 4 2 0
-4.0428 -4.0428 -7.4623 -7.4623 -2.1342 -2.1342 -6.45 -6.45
-0.1000 0.1000 0.1000 -0.1000 -0.1000 0.1000 0.1000 -0.1000
11.1969 11.1969 13.1794 13.1794 13.6397 13.6397 15.7900 15.7900
9.0 2.0 4.0 4.0 2.0 2.0
-1.0 -1.0 -1.0 -1.0 -1.0 -1.0
10 20 36 26 0 5 3 0
1.6125 1.6125 -1.6125 -1.6125 1.6125 1.6125 -1.6125 -1.6125
-1.6125 1.6125 1.6125 -1.6125 -1.6125 1.6125 1.6125 -1.6125
8.7400 8.7400 8.7400 8.7400 11.0900 11.0900 11.0900 11.0900
2.0 2.0 2.0 2.0 4.0 2.0
-1.0 -1.0 -1.0 -1.0 -1.0 -1.0
11 25 36 20 0 4 3 0
7.4623 7.4623 4.0428 4.0428 6.45 6.45 2.1342 2.1342
-1.6125 1.6125 1.6125 -1.6125 -1.6125 1.6125 1.6125 -1.6125
12.1150 12.1150 10.1850 10.1850 14.9150 14.9150 13.9650 13.9650
4.0 10.0 2.0 2.0 2.0 2.0
-1.0 -1.0 -1.0 -1.0 -1.0 -1.0
12 24 24 54 0 2 1 0
1.8250 1.8250 -1.8250 -1.8250 1.8250 1.8250 -1.8250 -1.8250
-1.8250 1.8250 1.8250 -1.8250 -1.8250 1.8250 1.8250 -1.8250
0.0 0.0 0.0 0.0 8.6150 8.6150 8.6150 8.6150
4.0 4.0 4.0 4.0 1.0 4.0
-1.0 -1.0 -1.0 -1.0 0.0 -1.0
13 24 24 7 0 2 1 0
1.8250 1.8250 -1.8250 -1.8250 1.8250 1.8250 -1.8250 -1.8250
-1.8250 1.8250 1.8250 -1.8250 -1.8250 1.8250 1.8250 -1.8250
8.6150 8.6150 8.6150 8.6150 8.6900 8.6900 8.6900 8.6900
4.0 4.0 4.0 4.0 4.0 1.0
-1.0 -1.0 -1.0 -1.0 -1.0 1.0

14 24 24 1 0 2 2 1
1.8250 1.8250 -1.8250 -1.8250 1.8250 1.8250 -1.8250 -1.8250
-1.8250 1.8250 1.8250 -1.8250 -1.8250 1.8250 1.8250 -1.8250
8.6900 8.6900 8.6900 8.6900 8.7400 8.7400 8.7400 8.7400
2.0 2.0 2.0 2.0 1.0 1.0
-1.0 -1.0 -1.0 -1.0 1.0 2.0
15 24 24 1 0 2 2 0
1.8250 1.8250 -1.8250 -1.8250 1.8250 1.8250 -1.8250 -1.8250
-1.8250 1.8250 1.8250 -1.8250 -1.8250 1.8250 1.8250 -1.8250
8.6900 8.6900 8.6900 8.6900 8.7400 8.7400 8.7400 8.7400
4.0 4.0 4.0 4.0 1.0 2.0
-1.0 -1.0 -1.0 -1.0 2.0 -1.0
16 20 20 54 0 2 1 0
1.4925 1.4925 -1.4925 -1.4925 1.4925 1.4925 -1.4925 -1.4925
-1.4925 1.4925 1.4925 -1.4925 -1.4925 1.4925 1.4925 -1.4925
0.0 0.0 0.0 0.0 8.6150 8.6150 8.6150 8.6150
4.0 4.0 4.0 4.0 1.0 4.0
-1.0 -1.0 -1.0 -1.0 0.0 -1.0
17 20 20 7 0 2 1 0
1.4925 1.4925 -1.4925 -1.4925 1.4925 1.4925 -1.4925 -1.4925
-1.4925 1.4925 1.4925 -1.4925 -1.4925 1.4925 1.4925 -1.4925
8.6150 8.6150 8.6150 8.6150 8.6900 8.6900 8.6900 8.6900
4.0 4.0 4.0 4.0 4.0 1.0
-1.0 -1.0 -1.0 -1.0 -1.0 1.0
18 20 20 1 0 2 2 1
1.4925 1.4925 -1.4925 -1.4925 1.4925 1.4925 -1.4925 -1.4925
-1.4925 1.4925 1.4925 -1.4925 -1.4925 1.4925 1.4925 -1.4925
8.6900 8.6900 8.6900 8.6900 8.7400 8.7400 8.7400 8.7400
2.0 2.0 2.0 2.0 1.0 1.0
-1.0 -1.0 -1.0 -1.0 1.0 2.0
19 20 20 1 0 2 2 0
1.4925 1.4925 -1.4925 -1.4925 1.4925 1.4925 -1.4925 -1.4925
-1.4925 1.4925 1.4925 -1.4925 -1.4925 1.4925 1.4925 -1.4925
8.6900 8.6900 8.6900 8.6900 8.7400 8.7400 8.7400 8.7400
4.0 4.0 4.0 4.0 1.0 4.0
-1.0 -1.0 -1.0 -1.0 2.0 -1.0
20 4 4 54 0 2 1 0
0.2990 0.2990 -0.2990 -0.2990 0.2990 0.2990 -0.2990 -0.2990
-0.2990 0.2990 0.2990 -0.2990 -0.2990 0.2990 0.2990 -0.2990
0.0 0.0 0.0 0.0 8.6150 8.6150 8.6150 8.6150
4.0 4.0 4.0 4.0 1.0 4.0
-1.0 -1.0 -1.0 -1.0 0.0 -1.0
21 4 4 7 0 2 1 0
0.2990 0.2990 -0.2990 -0.2990 0.2990 0.2990 -0.2990 -0.2990
-0.2990 0.2990 0.2990 -0.2990 -0.2990 0.2990 0.2990 -0.2990

8.6150 8.6150 8.6150 8.6150 8.6900 8.6900 8.6900 8.6900
4.0 4.0 4.0 4.0 4.0 1.0
-1.0 -1.0 -1.0 -1.0 -1.0 1.0
22 4 4 1 0 2 2 1
0.2990 0.2990 -0.2990 -0.2990 0.2990 0.2990 -0.2990 -0.2990
-0.2990 0.2990 0.2990 -0.2990 -0.2990 0.2990 0.2990 -0.2990
8.6900 8.6900 8.6900 8.6900 8.7400 8.7400 8.7400 8.7400
2.0 2.0 2.0 2.0 1.0 1.0
-1.0 -1.0 -1.0 -1.0 1.0 2.0
23 4 4 1 0 2 2 1
0.2990 0.2990 -0.2990 -0.2990 0.2990 0.2990 -0.2990 -0.2990
-0.2990 0.2990 0.2990 -0.2990 -0.2990 0.2990 0.2990 -0.2990
8.6900 8.6900 8.6900 8.6900 8.7400 8.7400 8.7400 8.7400
1.0 1.0 1.0 1.0 1.0 4.0
2.0 2.0 2.0 2.0 2.0 -1.0
24 4 4 26 0 5 2 1
0.2990 0.2990 -0.2990 -0.2990 0.2990 0.2990 -0.2990 -0.2990
-0.2990 0.2990 0.2990 -0.2990 -0.2990 0.2990 0.2990 -0.2990
8.7400 8.7400 8.7400 8.7400 14.0900 14.0900 14.0900 14.0900
1.0 1.0 1.0 1.0 4.0 2.0
2.0 2.0 2.0 2.0 -1.0 -1.0
25 24 44 54 0 2 1 0
1.8370 1.8370 -1.8370 -1.8370 1.8370 1.8370 -1.8370 -1.8370
-1.8370 1.8370 1.8370 -1.8370 -1.8370 1.8370 1.8370 -1.8370
0.0 0.0 0.0 0.0 8.6150 8.6150 8.6150 8.6150
4.0 4.0 4.0 4.0 1.0 4.0
-1.0 -1.0 -1.0 -1.0 0.0 -1.0
26 24 44 7 0 2 1 0
1.8370 1.8370 -1.8370 -1.8370 1.8370 1.8370 -1.8370 -1.8370
-1.8370 1.8370 1.8370 -1.8370 -1.8370 1.8370 1.8370 -1.8370
8.6150 8.6150 8.6150 8.6150 8.6900 8.6900 8.6900 8.6900
4.0 4.0 4.0 4.0 4.0 1.0
-1.0 -1.0 -1.0 -1.0 -1.0 5.0
27 24 44 1 0 2 3 1
1.8370 1.8370 -1.8370 -1.8370 1.8370 1.8370 -1.8370 -1.8370
-1.8370 1.8370 1.8370 -1.8370 -1.8370 1.8370 1.8370 -1.8370
8.6900 8.6900 8.6900 8.6900 8.7400 8.7400 8.7400 8.7400
2.0 2.0 2.0 2.0 1.0 1.0
-1.0 -1.0 -1.0 -1.0 5.0 6.0
28 24 44 1 0 2 3 0
1.8370 1.8370 -1.8370 -1.8370 1.8370 1.8370 -1.8370 -1.8370
-1.8370 1.8370 1.8370 -1.8370 -1.8370 1.8370 1.8370 -1.8370
8.6900 8.6900 8.6900 8.6900 8.7400 8.7400 8.7400 8.7400
4.0 4.0 4.0 4.0 1.0 2.0
-1.0 -1.0 -1.0 -1.0 6.0 -1.0

29 20 36 54 0 2 1 0
1.6125 1.6125 -1.6125 -1.6125 1.6125 1.6125 -1.6125 -1.6125
-1.6125 1.6125 1.6125 -1.6125 -1.6125 1.6125 1.6125 -1.6125
0.0 0.0 0.0 0.0 8.6150 8.6150 8.6150 8.6150
4.0 4.0 4.0 4.0 1.0 4.0
-1.0 -1.0 -1.0 -1.0 0.0 -1.0
30 20 36 7 0 2 1 0
1.6125 1.6125 -1.6125 -1.6125 1.6125 1.6125 -1.6125 -1.6125
-1.6125 1.6125 1.6125 -1.6125 -1.6125 1.6125 1.6125 -1.6125
8.6150 8.6150 8.6150 8.6150 8.6900 8.6900 8.6900 8.6900
4.0 4.0 4.0 4.0 4.0 1.0
-1.0 -1.0 -1.0 -1.0 -1.0 5.0
31 20 36 1 0 2 3 1
1.6125 1.6125 -1.6125 -1.6125 1.6125 1.6125 -1.6125 -1.6125
-1.6125 1.6125 1.6125 -1.6125 -1.6125 1.6125 1.6125 -1.6125
8.6900 8.6900 8.6900 8.6900 8.7400 8.7400 8.7400 8.7400
2.0 2.0 2.0 2.0 1.0 1.0
-1.0 -1.0 -1.0 -1.0 5.0 6.0
32 20 36 1 0 2 3 0
1.6125 1.6125 -1.6125 -1.6125 1.6125 1.6125 -1.6125 -1.6125
-1.6125 1.6125 1.6125 -1.6125 -1.6125 1.6125 1.6125 -1.6125
8.6900 8.6900 8.6900 8.6900 8.7400 8.7400 8.7400 8.7400
4.0 4.0 4.0 4.0 1.0 4.0
-1.0 -1.0 -1.0 -1.0 6.0 -1.0
33 4 4 54 0 2 1 0
0.3500 0.3500 -0.3500 -0.3500 0.3500 0.3500 -0.3500 -0.3500
-0.3500 0.3500 0.3500 -0.3500 -0.3500 0.3500 0.3500 -0.3500
0.0 0.0 0.0 0.0 8.6150 8.6150 8.6150 8.6150
4.0 4.0 4.0 4.0 1.0 4.0
-1.0 -1.0 -1.0 -1.0 0.0 -1.0
34 4 4 7 0 2 1 0
0.3500 0.3500 -0.3500 -0.3500 0.3500 0.3500 -0.3500 -0.3500
-0.3500 0.3500 0.3500 -0.3500 -0.3500 0.3500 0.3500 -0.3500
8.6150 8.6150 8.6150 8.6150 8.6900 8.6900 8.6900 8.6900
2.0 2.0 2.0 2.0 4.0 1.0
-1.0 -1.0 -1.0 -1.0 -1.0 5.0
35 4 4 1 0 2 3 1
0.3500 0.3500 -0.3500 -0.3500 0.3500 0.3500 -0.3500 -0.3500
-0.3500 0.3500 0.3500 -0.3500 -0.3500 0.3500 0.3500 -0.3500
8.6900 8.6900 8.6900 8.6900 8.7400 8.7400 8.7400 8.7400
2.0 2.0 2.0 2.0 1.0 1.0
-1.0 -1.0 -1.0 -1.0 5.0 6.0
36 4 4 1 0 2 3 1
0.3500 0.3500 -0.3500 -0.3500 0.3500 0.3500 -0.3500 -0.3500
-0.3500 0.3500 0.3500 -0.3500 -0.3500 0.3500 0.3500 -0.3500

```
8.6900 8.6900 8.6900 8.6900 8.7400 8.7400 8.7400 8.7400
1.0   1.0   1.0   1.0   1.0   4.0
6.0   6.0   6.0   6.0   6.0   -1.0
37  4  4 26  0  5  3  1
0.3500 0.3500 -0.3500 -0.3500 0.3500 0.3500 -0.3500 -0.3500
-0.3500 0.3500 0.3500 -0.3500 -0.3500 0.3500 0.3500 -0.3500
8.7400 8.7400 8.7400 8.7400 12.4650 12.4650 12.4650 12.4650
1.0   1.0   1.0   1.0   4.0   2.0
6.0   6.0   6.0   6.0   -1.0  -1.0
ncopy  13
12 38  1  2.0
13 39  1  2.0
14 40  2  2.0
15 41  2  2.0
16 42  1  2.0
17 43  1  2.0
18 44  2  2.0
19 45  2  2.0
20 46  1  2.0
21 47  1  2.0
22 48  2  2.0
23 49  2  2.0
24 50  2  2.0
tiltflag   0
pentflag   0
wedgeflag   0
translate   0
 nlocxy   0
 reshape  39
20 16  9  9  1  0
21 17  9  9  1  0
22 18  9  9  1  0
23 19  9  9  1  0
24  5  9  9  1  0
16 12  3  3  0  0
17 13  3  3  0  0
18 14  3  3  0  0
19 15  3  3  0  0
12  1 14  3  0  0
13  2 14  3  0  0
14  3 14  3  0  0
15  4 14  3  0  0
33 29  9 17  1  0
34 30  9 17  1  0
35 31  9 17  1  0
```

36	32	9	17	1	0
37	10	9	17	1	0
29	25	3	5	0	0
30	26	3	5	0	0
31	27	3	5	0	0
32	28	3	5	0	0
25	1	47	19	0	0
26	2	47	19	0	0
27	3	47	19	0	0
28	4	47	19	0	0
46	42	9	9	1	0
47	43	9	9	1	0
48	44	9	9	1	0
49	45	9	9	1	0
50	6	9	9	1	0
42	38	3	3	0	0
43	39	3	3	0	0
44	40	3	3	0	0
45	41	3	3	0	0
38	1	14	55	0	0
39	2	14	55	0	0
40	3	14	55	0	0
41	4	14	55	0	0

straightx0 0
straighty0 0
nlocxyz 808958
npentxy 0
nvguide 0
nvalvport 0
nrunner 0
nsiamese 0
nround 0
npatch 11

2	5	1	1	1	1
3	5	2	1	1	2
4	5	3	1	1	3
5	5	4	16	57	4
6	5	4	16	5	4
10	5	4	49	23	4
7	2	5	1	7	5
8	2	6	1	7	6
9	4	7	1	1	7
9	3	8	1	1	8
11	1	10	1	7	10

nrelaxb 0

nprovtop 0
nprovfce 0
nzcylwall 54
0.0000
0.1944
0.3889
0.5833
0.7778
0.9722
1.1667
1.3611
1.5556
1.7500
1.9444
2.1389
2.3333
2.5278
2.7222
2.9167
3.1111
3.3056
3.5000
3.6944
3.8889
4.0833
4.2778
4.4722
4.6667
4.8611
5.0556
5.2500
5.4444
5.6389
5.8333
6.0278
6.2222
6.4167
6.6111
6.8056
7.0000
7.1944
7.3889
7.5833
7.7778
7.9722

8.1667
8.3611
8.5556
8.7500
8.9444
9.1389
9.3333
9.5278
9.7222
9.9167
10.1111
10.3056
tilt 0
ndish 0
nscallop 0
xoffset 0.0
yoffset 0.0
write17 1.0
plotmesh 1.0
xband 0.1
yband 0.15
zband 0.01
nxplots 2
-2.00
+2.50
nyplots 2
0.0
1.95
nzplots 1
0.0
nvhide 2
45.0 75.0 5.0
225.0 115.0 5.0

B.2 Itape5

Ford 5.4L V8 Engine

irest 0

nohydro 1

lwall 1

lpr 0

irez 4

ncfilm 9999

nctap8 50

nclast 9999

ncmon 25

ncaspec 18

0.0, 15.0, 30.0, 60.0, 103.0, 180.0, 216.0, 270.0, 315.0, 345.0, 360.0,

405.0, 450.0, 495.0, 540.0, 630.0, 609.0, 720.0

gmv 1.0

cafilm 9.99e+9

cafin 720.0

angmom 0.0

pgssw 0.0

dti 1.00000e-5

dtmxca 1.0

dtmax 1.00000e-3

tlimd 1.0

twfilm 9.99e+9

twfin 9.99e+9

fchsp 0.25

bore 9.0216

stroke 9.9

squish 0.6

rpm 1.5e+3

atdc 0.0

datdct 0.0

revrep 2.0

conrod 16.91

swirl 0.0

swipro 3.11

thsect 360.0

sector 0.0

deact 0.0

epsy 1.0e-3

epsv 1.0e-3

epsp 1.0e-4

epst 1.0e-3

epsk 1.0e-3

epse 1.0e-3

gx 0.0

gy 0.0

gz 0.0

tcylwl 293.15

thead 293.15

tpistn 293.15

pardon 0.0

a0 0.0

b0 1.0

artvis 0.0

ecnsrv 0.0

adia 0.0

anu0 0.0

visrat-.66666667

tcut 1000.0

tcute 1200.0

epschm 0.02

omgchm 1.0

turbsw 1.0

sgsl 0.0

trbchem 0.0

capa 18.0

pmplict 0.0

lospeed 0.0

airmu1 1.457e-5

airmu2 110.0

airla1 252.0

airla2 200.0

prl 0.74

rpr 1.11

rsc 1.11

xignit 9.0e+9

tlign -9.99e+9

tdign -9.99e+9

calign -13.5

cadign 10.0

xignl1 0.0

xignr1 0.0

yignf1 0.0

yignd1 0.0

zignb1 0.0

zignt1 0.0

xignl2 0.0

xignr2 0.0

yignf2 0.0

yignd2 0.0

zignb2 0.0

zignt2 0.0

kwikeq 1

numnoz 1

numinj 1

numvel 1

t1inj -9.99e+9

tdinj -9.99e+9

ca1inj -300.0

cadinj 48.0

tspmas 0.015

tnparc 1000.0

pulse 2.0

injdist 1

kolide 1

tpi 293.15

turb 1.0

breakup 1.0

evapp 1.0

drnoz +2.6

dznoz 10.97

dthnoz 180.0

tiltxy 0.0

tiltxz 35.0

cone 60.0

dcone 60.0

anoz 1.0

smr 1.50e-3

amp0 0.0

1400.0

nsp 12

gasoline

o2 mw2 32.000 htf2 0.0

n2 mw3 28.016 htf3 0.0

co2 mw4 44.011 htf4 -93.965

h2o mw5 18.016 htf5 -57.103

h mw6 1.008 htf6 51.631

h2 mw7 2.016 htf7 0.0

o mw8 16.000 htf8 58.989

n mw9 14.008 htf9 112.520

oh mw10 17.008 htf10 9.289

co mw11 28.011 htf11 -27.200

no mw12 30.008 htf12 21.456

stoifuel 4.0

stoio2 49.0

```
nreg     1

presi,    3*6.0000e+5

tempi,    3*293.15

tkei,     3*0.10

scli,     3*0.0

er,       3*0.0

mfracfu,  3*0.0

mfraco2,  3*0.2200910204

mfracn2,  3*0.7650385386

mfracco2, 3*9.913863271e-3

mfrach2o, 3*4.956577746e-3

mfrach,   3*0.0

mfrach2,  3*0.0

mfraco,   3*0.0

mfracn,   3*0.0

mfracoh,  3*0.0

mfracco,  3*0.0

mfracno,  3*0.0

nrk     4

cf1  8.0000e10 ef1  1.5780e+4 zf1     0.0

cb1     0.0   eb1     0.0   zb1     0.0

am1    4  49  0  0  0  0  0  0  0  0  0  0
```

bm1 0 0 0 32 34 0 0 0 0 0 0 0

ae1 0.250 1.500 0.000 0.000 0.000 0.000 0.000 0.000

0.000 0.000 0.000 0.000

be1 0.000 0.000 0.000 0.000 0.000 0.000 0.000 0.000

0.000 0.000 0.000 0.000

cf2 1.5587e14 ef2 6.7627e+4 zf2 0.0

cb2 7.5000e12 eb2 0.0 zb2 0.0

am2 0 1 2 0 0 0 0 0 0 0 0 0

bm2 0 0 0 0 0 0 0 0 2 0 0 2

ae2 0.000 0.500 1.000 0.000 0.000 0.000 0.000 0.000

0.000 0.000 0.000 0.000

be2 0.000 0.000 0.000 0.000 0.000 0.000 0.000 0.000

1.000 0.000 0.000 1.000

cf3 2.6484e10 ef3 5.9418e+4 zf3 1.0

cb3 1.6000e+9 eb3 1.9678e+4 zb3 1.0

am3 0 2 1 0 0 0 0 0 0 0 0 0

bm3 0 0 0 0 0 0 0 2 0 0 0 2

ae3 0.000 1.000 0.500 0.000 0.000 0.000 0.000 0.000

0.000 0.000 0.000 0.000

be3 0.000 0.000 0.000 0.000 0.000 0.000 0.000 1.000

0.000 0.000 0.000 1.000

cf4 2.1230e14 ef4 5.7020e+4 zf4 0.0

cb4 0.0 eb4 0.0 zb4 0.0

am4 0 0 1 0 0 0 0 0 0 2 0 0

bm4 0 0 0 0 0 2 0 0 0 0 0 2

ae4 0.000 0.000 0.500 0.000 0.000 0.000 0.000 0.000

0.000 1.000 0.000 0.000

be4 0.000 0.000 0.000 0.000 0.000 1.000 0.000 0.000

0.000 0.000 0.000 1.000

nvalves 3

vliftmin 0.05

skirtth 0.1

tmove 293.15

vtiltxz -5.8

nlift 139

vliftmin 0.05

skirtth 0.1

tmove 293.15

vtiltxz -5.8

nlift 140

vliftmin 0.05

skirtth 0.1

tmove 293.15

vtiltxz +5.1

nlift 140

isoot 0

distamb 2.0

pamb 9.9000e+5

tkeamb 423.0

sclamb 4.8

velin 0.0

reedin 0.0

reedout 0.0

nregin0 2

nregamb 3

numpcc 2

0.0 9.9000e+5

720.0 9.9000e+5

numpex 2

0.0 9.9000e+5

720.0 9.9000e+5

BIBLIOGRAPHY

BIBLIOGRAPHY

1. Zhao F.-Q., Lai M.-C., and Harrington D. L. A Review of Mixture Preparation and Combustion Control Strategies for Spark-Ignited Direct-Injection Gasoline Engines SAE Paper 970627.

2. Harada J., Tomita T., Mizuno H., Mashiki Z., and Ito Y. Development of a Direct Injection Gasoline Engine SAE Paper 970540.

3. Tomoda T., Sasaki S., Sawada D., Saito A., and Sami H. Development of Direct Injection Gasoline Engine – Study of Stratified Mixture Formation SAE Paper 970539.

4. Han Z., Fan L., and Reitz R. D. Multidimensional Modeling of Spray Atomization and Air/Fuel Mixing in a Direct-Injection Spark-Ignition Engine SAE Paper 970884.

5. David L.S. Hung, Guoming G. Zhu, James R. Winkelman Tom Stuecken, Harold Schock and Andrew Fedewa, A High Speed Flow Visualization Study of Fuel Spray Pattern Effect on Mixture Formation in a Low Pressure Direct Injection Gasoline Engine SAE Paper 07PFL-662

6. Hansgert Hascher, The Influence of Speed, Stroke and Load Variations on the Major In-Cylinder Flow Patterns of a Four-Vlave Spark-Ignition Engine, Doctoral dissertation RWTH-Aachen, 1999

7. Edward S. Suh and Christopher J. Rutland Numerical Study of Fuel/Air Mixture Preparation in a GDI Engine SAE Paper 1999-01-3657

8. Rolf Reitz, Development of IC Engine Modeling , invited speech, Engine Research Lab, MSU, 2003

9. Donald W.Stanton, Christopher J.Rutland, Multi-Dimensional Modeling of Heat and Mass Transfer of Fuel Films Ressulting From Impinging Sprays , SAE Paper 980312

10. Satpreet Nanda, Song-Lin Yang , IC ngine Flow Simulation using KIVA code and A Modified Reynolds Stress Turbulence Model KIVA3-V modeling meeting, University of Wisconsin-Madison, 2004

11. CHEN YEN TEO, CFD Study Of Discrete Jet LDI Combustor Using KIVA Code With Re-Stress Model, Degree thesis, 2002

12. Amsden "KIVA-3: A KIVA Program with Block-Structured Mesh for Complex

Geometries" Los Alamos National Lab 1989

13. Amsden "KIVA-3: A KIVA Program with Block-Structured Mesh for Complex Geometries" Los Alamos National Lab 1993

14. Amsden "KIVA-3: "KIVA-3V: A Block-Structured KIVA Program for Engines with Vertical or Canted Valves Los Alamos National Lab, 1997

15. GRIDGEN User Maunal (Version 15.0), Pointwise Inc, 2004

16. GRIDGEN Tutorial (Version 15.0), Pointwise Inc, 2004

17. Frank P. Incropera, David P. Dewitt, Fundamentals of Heat and Mass Transfer, 5th Edition Hemisphere Publishing

18. Amsden "KIVA-3: "KIVA-3V: A Block-Structured KIVA Program for Engines with Vertical or Canted Valves release2 Los Alamos National Lab, 1998

19. James Yi, Rapid Mesh Generation and Dynamic Mesh Management for KIVA-3V, KIVA3-V modeling meeting, University of Wisconsin-Madison, 2002

20. Tecplot 10.0 User Manual and Tutorial, Tecplot Inc,2005

21. John Heywood, Fundamentals of Internal Combustion engines McGraw Hill, 1988